Final Report

COMPARATIVE ANALYSIS OF FINE SCALE SATELLITE & REANALYSIS PRECIPITATION ESTIMATES IN UPPER GANGA BASIN USING MULTICRITERION DECISION-MAKING

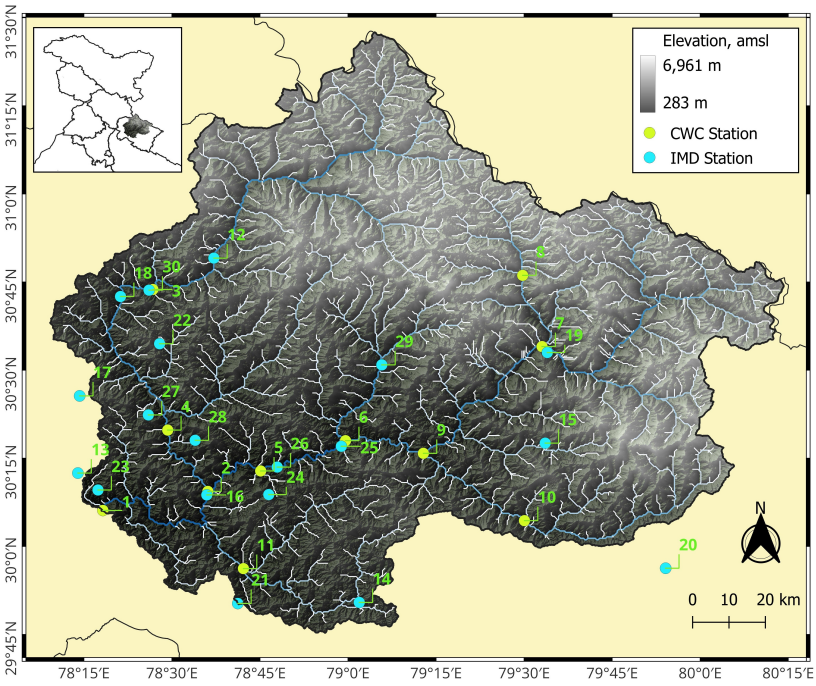

Centre for Cryosphere and Climate Change Studies

National Institute of Hydrology

March 2023

Director

Dr. M.K. Goel

Head

Dr. Surjeet Singh

Study Group

Dr. D.S. Bisht (Scientist 'C')

Dr. M.K. Goel (Scientist 'G')

Abstract

Precipitation is a crucial variable in hydrological studies, significantly affecting their outcomes. In mountainous regions, the complex topography hinders the establishment of dense networks of weather stations, and even if such networks were possible, historical data gaps would remain. Historical records are essential for understanding changes in local hydrological patterns, yet the increasing reliance on satellite and reanalysis data has reduced dependence on ground-based stations. Satellite Precipitation Estimates (SPEs) and Reanalysis Precipitation Estimates (RPEs) are widely used, but their accuracy varies across regions, necessitating rigorous assessment through statistical methods to determine their effectiveness in capturing regional precipitation patterns.

This study evaluates five Precipitation Estimates (PEs): two SPEs (IMERG and CHIRPS), two RPEs (ERA5-Land and IMDAA), and the IMD gridded product, in representing precipitation climatology in the Upper Ganga Basin (UGB). These products were compared with rainfall data from 30 gauges (19 from the India Meteorological Department and 11 from the Central Water Commission) over 18 hydrological years (May 2000–June 2018). Performance was assessed using Normalized Root Mean Square Deviation (NRMSD), Pearson Correlation Coefficient (CC), and Skill Score (SS). Five multicriterion decision-making (MCDM) methods—Compromise Programming (CP), Cooperative Game Theory (CGT), Technique for Order of Preference by Similarity to Ideal Solution (TOPSIS), Weighted Average Technique (WAT), and Fuzzy TOPSIS—were applied to rank the PEs. Weights for NRMSD, CC, and SS were determined using an entropy-based method. A Group Decision Making (GDM) approach, incorporating Spearman correlation and an additive ranking rule, was used to integrate the MCDM rankings.

The results show that IMERG is the most suitable SPE, outperforming CHIRPS, while ERA5-Land is a superior RPE compared to IMDAA. Expectedly, the IMD gridded data which is developed using station observation performed with

greater accuracy for a large number of sttaions. IMDAA was found to be least suitable PE for the UGB, followed by CHIRPS among the analyzed five PEs. The full report details the methodology and results.

Keywords: Upper Ganga Basin, ERA5, IMDAA, IMERG, CHIRPS, IMD, MCDM, GDM

Contents

List of Figures

List of Tables

List of Abbreviations

CC	Pearson Correlation Coefficient
CGT	Cooperative Game Theory
CHIRPS	Climate Hazards Group InfraRed Precipitation with Station data
CP	Compromised Programming
CWC	Central Water Commission
ECMWF	European Centre for Medium-Range Weather Forecasts
ERA5	ECMWF Reanalysis v5
GDM	Group Decision-making
GPM	Global Precipitation Measurement
IMD	India Meteorological Department
IMDAA	Indian Monsoon Data Assimilation and Analysis
IMERG	Integrated Multi-satellitE Retrievals for GPM
MCDM	Multicriterion Decision-making
NCMRWF	National Center For Medium Range Weather Forecasting
NRMSD	Normalized Root Mean Square Deviation
PE	Precipitation Estimate
RPE	Reanalysis Precipitation Estimate

List of Abbreviations

SPE	Satellite Precipitation Estimate
SS	Skill Score
TOPSIS	Technique for Order Preference by Similarity to an Ideal Solution
UGB	Upper Ganga Basin
WAT	Weighted Average Technique

Chapter 1

Introduction

1.1 Background

Precipitation plays a critical role in agriculture, water supply, and overall livelihoods. However, accurately quantifying precipitation at sub-regional and local levels is challenging due to its erratic nature and skewed distribution, especially within the complex mountainous terrain of the Himalayas (Meher et al., 2017). In any hydrological analysis of a river basin, the foremost task is the collection of accurate, consistent, and continuous rainfall data. Given the involvement of multiple organizations in India in collecting hydrological and meteorological data, it is essential to integrate this information, particularly related to precipitation. Beyond point observations, various global and regional datasets offer spatial precipitation information across different temporal scales, and these datasets are publicly accessible Bisht et al. (2024); Chowdhury et al. (2021); Singh et al. (2024).

The steep topography of the Himalayan region significantly influences the climate and weather patterns across the country, serving as a primary water source for the Indo-Gangetic plains through rainfall and snow/glacial melt. In many parts of the Himalayas, ecological and hydrological data are either unavail-

able or plagued by issues such as inconsistencies and missing records. As a result, processing this data to assess hydrological and ecological conditions in the region is a complex task. Raw hydrological data typically require processing before they can be used effectively in analysis, with the two primary objectives being to verify the data's accuracy and to format it for practical use. Advances in computing technology, particularly in processing speed, data storage capacity, and hydrological software capabilities, have significantly simplified the management of large volumes of hydrological data. Tools like the Surface Water Data Entry System (SWDES), developed under the Hydrology Project – I Consultants & Hydraulics (1999), and HYMOS software (Hydraulics, 1999), can be readily employed to manage and process the hydrological database.

In mountainous regions, the substantial variation in altitude, slope, aspect, soil, and land use over short distances necessitates a dense hydrometric network for reliable water resource assessment. However, operational challenges have hindered the establishment of an adequate observation network in these areas. Moreover, global concerns about climate change and its impacts on hydrological variables are particularly pertinent to mountainous regions, which are considered more vulnerable to these changes IPCC (2023). Consequently, there is a pressing need to design and upgrade hydro-meteorological networks in the region for long-term monitoring. Additionally, identifying secondary data sources that provide extensive temporal coverage and seamless spatial information is crucial. Such data can be instrumental in analyzing water scenarios and developing strategies for effective water resource management.

It is well documented that the hydro-meteorological station network in the Himalayan region is sparse, and harsh climatic conditions further complicate the maintenance of quality data records Bisht et al. (2024). This data scarcity presents a significant challenge in analyzing the hydro-meteorological dynamics in the context of a changing climate. However, technological advancements have reduced the need for manual intervention and station-based data recording, leading to the development of numerous global gridded products by researchers worldwide using sophisticated techniques. Additionally, remotely sensed data from satellite observations have become increasingly available in recent years. These global

datasets, which are openly accessible, have been widely utilized in various studies. While the importance of station-based observations remains significant, global datasets are invaluable for understanding historical climate patterns and changes over time, as well as for real-time applications. Some of the most widely used open datasets available at very fine spatial resolution include CHIRPS, GPM-IMERG, ERA5, and IMDAA. These datasets, covering different time periods and developed using various techniques and algorithms, are particularly important in the context of the data scarcity in the Himalayan region. It is therefore crucial to evaluate the global datasets available from various satellites and products to address these gaps.

1.2 Problem Definition

Examining rainfall patterns in the Himalayan region is critical, as the livelihoods of over half a billion people and the region's rich biodiversity are heavily dependent on meltwater from the Himalayas (Meher et al., 2017). Despite this importance, obtaining accurate climate change data for the Himalayas remains difficult due to the region's complex topography, limited data availability, and the often poor quality of existing data (Andermann et al., 2011; Arora et al., 2006; Bhutiyani et al., 2007; Dimri & Dash, 2012; Palazzi et al., 2013; Singh et al., 2009, 1995). Long-term rainfall records are essential for conducting various statistical analyses in climate change studies, as they provide robust estimates of distribution parameters such as scale, shape, and location, which are crucial for quantile mapping and frequency analysis.

The Upper Ganga Basin (UGB) is a crucial catchment within the Indian Himalayan Region (IHR), encompassing the Bhagirathi and Alaknanda rivers, which merge at Devprayag to form the Ganga River. A significant portion of the UGB is covered by snow, contributing to climate feedback mechanisms and maintaining river flow during lean seasons through snow and glacier melt. To

accurately understand the hydrological dynamics of the UGB, it is vital to have precise precipitation data for the region. However, capturing accurate precipitation data at sub-regional and local scales is challenging due to the erratic nature of precipitation patterns and skewed statistics, especially in mountainous terrain.

Climate change studies require long-term rainfall records for statistical analyses. These records are crucial for obtaining reliable estimates of distribution parameters like scale, shape, and location, which are used in quantile mapping, frequency analysis, and other hydrological applications. Consequently, long-term time series data, rather than shorter-interval satellite rainfall information, are essential. Various precipitation products exist for different timeframes, and a single source rarely provides comprehensive coverage. In such cases, combining information from multiple products based on their performance is necessary. However, prior to combining datasets, it is essential to evaluate and rank their performance to avoid erroneous selections. When utilizing any global dataset for the UGB, it is crucial to assess its ability to accurately represent the region's precipitation climatology and capture extreme events. A thorough statistical approach is required for these evaluations, which involves assessing the accuracy of various precipitation estimates in both temporal and spatial dimensions and ranking their performance Bisht et al. (2024); Chowdhury et al. (2021), thus aiding hydrological research .

1.3 Objectives of the study

The present study aims to evaluate the selected Precipitation Estimates (PEs) derived from satellite and reanalysis products i.e., Satellite Precipitation Estimates (SPEs) and Reanalysis Precipitation Estimates (RPEs) for Upper Ganga Basin (UGB) and rank them as per their skills in resolving the precipitation climatology. Keeping this in view, the following objectives were laid for the study,

1. To perform statistical evaluation of fine scale satellite and reanalysis precip-

itation products in Upper Ganga Basin vis-à-vis station records.

2. To estimate performance ranking of fine scale satellite and reanalysis precipitation product in Upper Ganga Basin using Multicriterion Decision-Making and Group Decision-Making.

1.4 Chapterization

This report is structured and organized into five chapters as follows,

Chapter-1 presents an overview of the study, problem statement and specifies the major objectives. It also summaries the organization of the report.

Chapter-2 provides the description of study area i.e., Upper Ganga Basin (UGB) in brief. It also discusses the various Precipitation Estimates (PEs) i.e., Satellite Precipitation Estimates (SPE), Reanalysis Precipitation Estimates (RPE) and observed gridded precipitation product developed by India Meteorological Data (IMD) in context of study area.

Chapter-3 describes the methodology and various performance indicators used in the study for statistical evaluation of PEs and their ranking for the study area. It provides the description on Multi Criteria Decision Making (MCDM) and Group Decision Making (GDM) for obtaining the ranks based on different performance criterion.

Chapter-4 presents the results of analysis pertaining to PEs ranking and their evaluation in detail with figures, spatial maps, and tables.

Chapter-5 summarizes the report in brief and presents the key conclusion drawn from the study. It also presents the limitation of the present work and scope for future study.

Chapter 2

Study Area and Data Used

2.1 Description of Study area

The present study focuses on the Upper Ganga Basin (UGB) up to Rishikesh, spanning latitudes from 29°45' N to 31°27' N and longitudes from 78°09' E to 80°15' E (Figure 2.1). The UGB covers a geographical area of ∼21,762 km^2, predominantly situated in mountainous terrain. The basin exhibits significant variations in both elevation and climate, with altitudes ranging from ∼283 m in the lower regions to ∼6,961 m in the higher mountains, as derived from the Cartosat v3r1 DEM. The climate of the UGB is primarily characterized by tropical and subtropical temperature zones. Three major topo-climatic regimes, influenced by regional topography, contribute to significant variability in monsoon precipitation, with annual averages ranging from 550 mm to 2500 mm (Basistha et al., 2008; Bookhagen & Burbank, 2010; Yadav et al., 2020). The southwest monsoon, occurring between July and late September, accounts for the majority of the region's rainfall. Notably, areas above 2500 m above mean sea level (amsl) are subject to significant snow cover and considerable winter snowfall. Rainfall distribution is uneven across the basin, with peripheral regions experiencing higher precipitation

compared to the central areas, reflecting the topographical influence as one moves from south to north. The Gangotri glacier, covering approximately 256 km^2, is the largest glacier within the basin (Yadav et al., 2020).

The Upper Ganga Basin comprises two main headwaters originating in the Himalayas: the Bhagirathi and Alaknanda river systems. The Bhagirathi river originates from the Gangotri glacier at Gomukh, while the Alaknanda river originates at the confluence of the Satopanth and Bhagirath Kharak glaciers in Uttarakhand. These rivers converge at Devprayag to form the main Ganga river, which flows through the Himalayas and emerges at Rishikesh, before descending onto the plains at Haridwar. The stream network of the UGB, including major rivers and the locations of CWC and IMD gauging stations, is illustrated in Figure 2.1. The Bhagirathi and Alaknanda rivers are primarily sustained by rainfall, springs (base flow), glacier melt, and snowmelt (Mishra et al., 2022). As such, precipitation data is critical for analyzing the region's water budget, facilitating informed decision-making, and addressing key hydrological questions.

The UGB comprises eight administrative districts, including Rudraprayag, parts of Uttarkashi, Chamoli, Tehri Garhwal, Pauri Garhwal, Bageshwar, and Pithoragarh in Uttarakhand, and Kinnaur district in Himachal Pradesh. However, the majority of the study area is dominated by five key districts: Uttarkashi, Rudraprayag, Chamoli, Tehri Garhwal, and Pauri Garhwal. Due to the rugged mountainous terrain and extensive inhospitable high-altitude regions, the population density in the UGB is relatively low. Approximately 85% of the population relies on rainfed agriculture and animal husbandry for their livelihood, while the remaining 15% are engaged in small businesses and labor. The basin is home to over 5,000 villages with a population of 25.69 million. The Tehri dam, India's highest dam at 260.5 m, is located on the Bhagirathi River in the Tehri Garhwal district.

Serial	Station
1	GG000Y4-RISHIKESH
2	GG100A1-DEOPRAYAG
3	GG100K4-UTTARKASHI
4	GG110A1-KOTESWAR
5	GG200B5-SRINAGAR
6	GG200G5-RUDRAPRAYAG
7	GG200S3-JOSHIMATH
8	GG200V5-BADRINATH
9	GG260A1-KARANPRAYAG
10	GG260J4-NANDKESHRI
11	GGZ00D3-MARORA
12	BHATWARI
13	BHOGPUR
14	BIRONKHOL
15	CHAMOLI
16	DEOPRAYAG
17	DHANOLTI
18	DUNDA
19	JOSHIMATH
20	KEERTINAGAR
21	LANDSDOWN
22	MUKHIM
23	NARENDRANAGAR
24	PAURI
25	RUDRAPRAYAG
26	SRINAGAR
27	TEHRI
28	TEHRI GARHWAL
29	OKHIMATH
30	UTTARKASHI

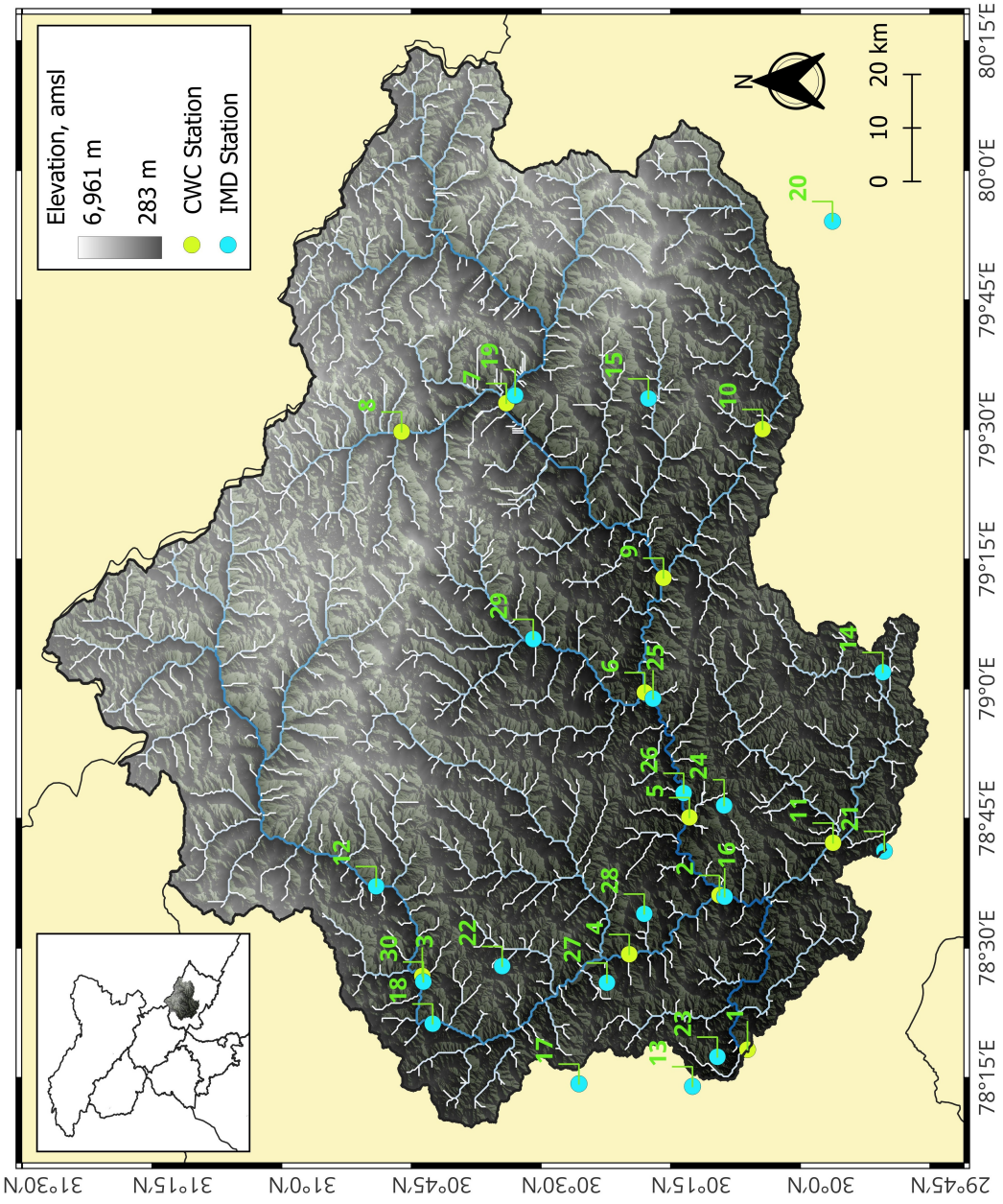

Figure 2.1: Map of the Upper Ganga Basin.

2.2 Description of Data Used

2.2.1 Station data

Precipitation records from 47 observatories of India Meteorological Department (IMD) and 11 gauges of Central Water Commission (CWC) in the Upper Ganga Basin (UGB) with varying length of were collected and scrutinized for missing data. A correlation analysis was performed to maximize data utilization, identifying stations with similar rainfall characteristics. A correlation matrix was developed to determine the relationships between stations, enabling the use of correlated stations for data validation and gap-filling using the normal-ratio method. Details of the precipitation data processing for CWC and IMD stations are discussed in a previously published report by the National Institute of Hydrology (NIH, 2022), and therefore are not elaborated upon here.

A total of 30 meteorological stations record were selected for further analysis following data processing. Of these, 19 were operated by the IMD, and 11 by the CWC. As shown in Table 2.1, the stations are distributed across a wide altitudinal range, from approximately 294 m above mean sea level (amsl) to 3136 m amsl. Thirteen stations are located below 1000 m amsl, 13 between 1000 and 2000 m amsl, and 4 above 2000 m amsl.

2.2.2 Precipitation Estimates

Precipitation Estimates (PEs) are available from a variety of sources, offering extensive temporal coverage and continuous spatial data over large regions. Unlike station data, which are point-specific and often sparsely distributed, PEs provide precipitation information at a grid scale in seamless manner with varying spatial resolutions. These estimates are particularly advantageous for precipita-

Table 2.1: Description of station

S. No.	Station	Source	Latitude	Longitude	Altitude (m, amsl)
1	GG000Y4-Rishikesh	CWC	30°06'07" N	78°18'14" E	294
2	GG100A1-Deoprayag	CWC	30°09'22" N	78°36'07" E	425
3	GG100K4-Uttarkashi	CWC	30°43'44" N	78°26'46" E	1093
4	GG110A1-Koteswar	CWC	30°19'48" N	78°29'17" E	603
5	GG200B5-Srinagar	CWC	30°12'50" N	78°45'07" E	511
6	GG200G5-Rudraprayag	CWC	30°18'00" N	78°59'35" E	678
7	GG200S3-Joshimath	CWC	30°34'01" N	79°33'04" E	1390
8	GG200V5-Badrinath	CWC	30°46'08" N	79°29'46" E	3136
9	GG260A1-Karanprayag	CWC	30°15'50" N	79°12'50" E	748
10	GG260J4-Nandkeshri	CWC	30°04'23" N	79°30'04" E	1162
11	GGZ00D3-Marora	CWC	29°56'13" N	78°42'11" E	512
12	Bhatwari	IMD	30°49'05" N	78°37'08" E	1566
13	Bhogpur	IMD	30°12'29" N	78°13'59" E	657
14	Bironkhol	IMD	29°50'28" N	79°01'55" E	1447
15	Chamoli	IMD	30°17'35" N	79°33'36" E	2628
16	Deoprayag	IMD	30°08'46" N	78°35'56" E	451
17	Dhanolti	IMD	30°25'37" N	78°14'17" E	2167
18	Dunda	IMD	30°42'32" N	78°21'14" E	1022
19	Joshimath	IMD	30°33'00" N	79°33'58" E	2063
20	Keertinagar	IMD	29°56'17" N	79°54'07" E	1076
21	Landsdown	IMD	29°50'17" N	78°41'13" E	1655
22	Mukhim	IMD	30°34'30" N	78°27'54" E	1817
23	Narendranagar	IMD	30°09'36" N	78°17'24" E	977
24	Pauri	IMD	30°08'49" N	78°46'30" E	1637
25	Rudraprayag	IMD	30°17'02" N	78°58'52" E	669
26	Srinagar	IMD	30°13'30" N	78°47'56" E	516
27	Tehri	IMD	30°22'23" N	78°25'59" E	1737
28	Tehri Garhwal	IMD	30°18'04" N	78°33'58" E	983
29	Okhimath	IMD	30°30'54" N	79°05'46" E	1380
30	Uttarkashi	IMD	30°43'37" N	78°26'06" E	1093

tion analysis, as they are not subject to the missing observations and consistency issues that often affect station records. Of late, Satellite Precipitation Estimates (SPEs) and Reanalysis Precipitation Estimates (RPEs) have become widely used for analyzing regional precipitation climatology and extreme events, as well as for modeling studies. In this study, SPEs such as IMERG and CHIRPS, along with two RPEs, namely ERA5-Land and IMDAA, have been assessed for their suitability in comparison to station data. Additionally, the IMD gridded precipitation data, available at a 25 km (0.25° x 0.25°) spatial resolution, is also utilized to evaluate its consistency with station observations. A brief overview of these datasets is provided below.

2.2.2.1 Satellite Precipitation Estimates (SPEs)

IMERG: Integrated Multi-satellitE Retrievals for GPM

The IMERG precipitation estimates utilizes data from constellation of GPM (Global Precipitation Measurement) satellites to derive the large scale precipitation information at i km (0.1° x 0.1°) spatial resolution (Huffman et al., 2015). The GPM is an international network of satellites that provide the next-generation global observations of rain and snow. GPM, initiated by NASA and the Japan Aerospace Exploration Agency (JAXA) as a global successor to TRMM, comprises a consortium of international space agencies, including the Centre National d'Études Spatiales (CNES), the Indian Space Research Organization (ISRO), the National Oceanic and Atmospheric Administration (NOAA), the European Organization for the Exploitation of Meteorological Satellites (EUMETSAT), and others.

The GPM Core Observatory carries the first space-borne Ku/Ka-band Dual-frequency Precipitation Radar (DPR) and a multi-channel GPM Microwave Imager (GMI). The DPR instrument, which provides three dimensional measurements of precipitation structure over 78 and 152 $mile$ (125 and 245 km) swaths, consists of a Ka-band precipitation radar (KaPR) operating at 35.5 GHz and a Ku-band precipitation radar (KuPR) operating at 13.6 GHz. Relative to the

TRMM precipitation radar, the DPR is more sensitive to light rain rates and snowfall. In addition, simultaneous measurements by the overlapping of Ka/Ku-bands of the DPR can provide new information on particle drop size distributions over moderate precipitation intensities. Utility and applicability of IMERG estimates have been demonstrated by many researchers across the globe (Beria et al., 2017; Cui et al., 2020; Li et al., 2021). The product which was initially made available year 2014 onward was later extended to cover the period of year 2000- 2014 using TRMM (Tropical Rainfall Measuring Mission) satellite data. In this study, the IMERG (version 06) data available at daily temporal resolution has been employed. Spatial distribution of selected stations and corresponding grids of IMERG is shown in Figure 2.2.

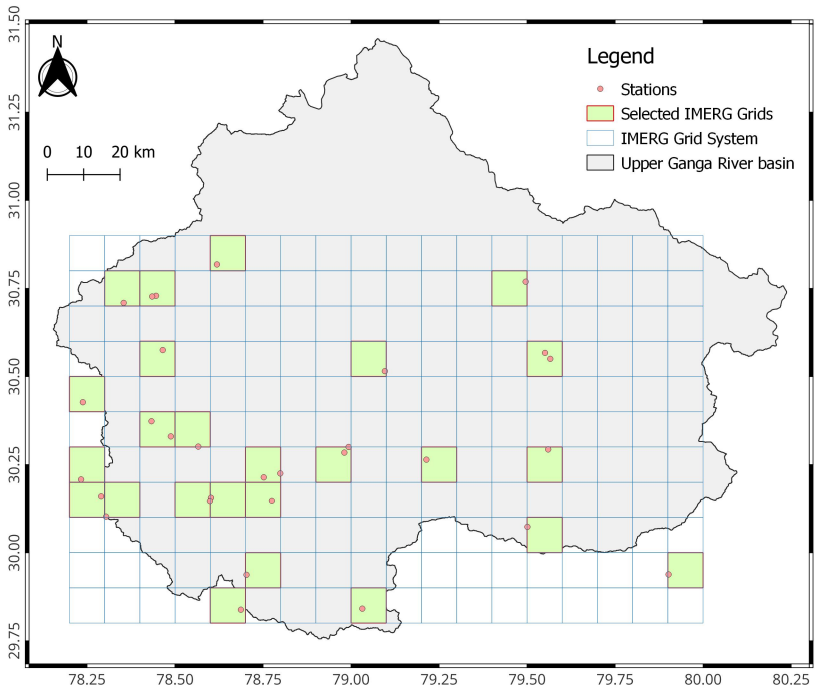

Figure 2.2: Distribution of IMERG grids and selected stations in UGB.

CHIRPS: Climate Hazards Group InfraRed Precipitation with Station data

The CHIRPS is a 30+ year quasi-global rainfall dataset. Spanning 50°S-50°N (and all longitudes), starting in 1981 to near-present (Funk et al., 2015).

CHIRPS incorporates 5 km (0.05° x 0.05°) resolution satellite imagery with in-situ station data to create gridded rainfall time series. CHIRPS uses the Tropical Rainfall Measuring Mission Multi-satellite Precipitation Analysis version 7 (TMPA 3B42 v7) to calibrate global Cold Cloud Duration (CCD) rainfall estimates. CHIRPS uses a 'smart interpolation' approach, working with anomalies from a high resolution climatology. CHIRPS incorporates station data in a two phase process, producing two unique products. In the first phase, which yields a preliminary rainfall product with 2-day latency, sparse World Meteorological Organization's Global Telecommunication System (GTS) gauge data are blended with CCD-derived rainfall estimates at every pentad. There are six pentads in a calendar month, five 5-day pentads and one pentad with the remaining 3 to 6 days of the month. In the second phase, which yields a final product with a $\sim$ 3 week latency, the best available monthly (and pentadal) station data are combined with monthly (and pentadal) high resolution CCD-based rainfall estimates to produce fields that are similar to gridded monthly station products like those produced by the Global Precipitation Climatology Centre (GPCC), or University of East Anglia's Climate Research Unit (CRU). Thus, the CHIRPS falls somewhere between heavily curated interpolated gauge datasets like the GPCC and sparse gauge plus satellite products like the RFE2.

Numerous works have demonstrated the applicability of CHIRPS dataset in the recent years (Bhattacharyya et al., 2022; Cavalcante et al., 2020; Wang et al., 2021; Yu et al., 2020a,b). Present study utilizes the CHIRPS daily dataset at 0.05° spatial resolution over the study area for the analysis. Spatial distribution of selected stations and corresponding grids of IMERG is shown in Figure 2.3.

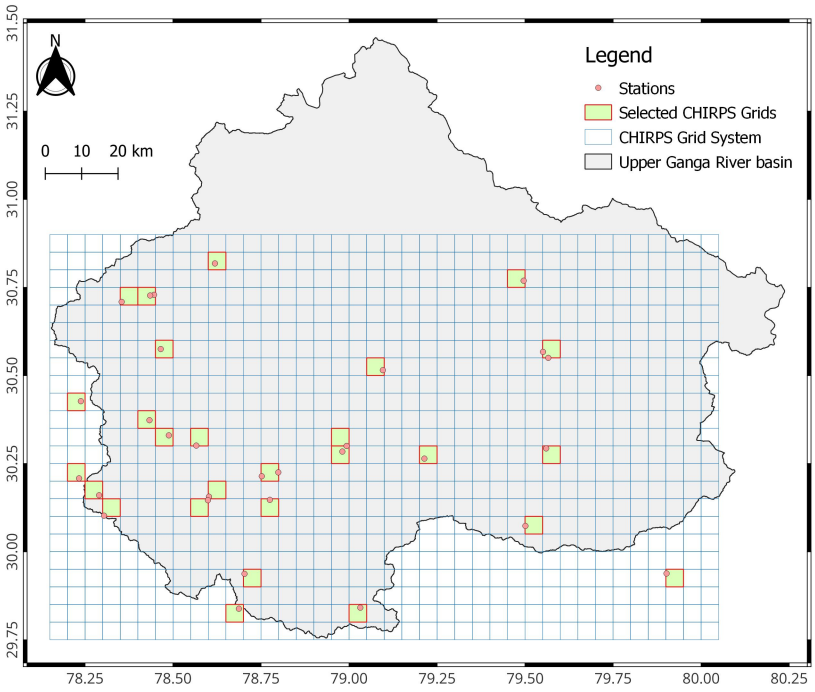

Figure 2.3: Distribution of CHIRPS grids and selected stations in UGB.

2.2.2.2 Reanalysis Precipitation Estimates (RPEs)

ERA5-Land

The ERA5-Land dataset provides a high-resolution reanalysis of land surface variables, offering a consistent representation of their evolution over several decades. With a spatial resolution of 10 km (0.1° x 0.1°), ERA5-Land integrates model data with global observations, applying physical laws to generate a comprehensive and coherent dataset. By using ERA5 atmospheric variables as inputs, ERA5-Land simulates land fields, incorporating observations indirectly through atmospheric forcing. This dataset delivers precise reconstructions of historical climate conditions, making it particularly useful for land surface applications, including flood and drought forecasting. While some uncertainties remain in the estimates, the high temporal and spatial resolutions of ERA5-Land render it an invaluable resource for researchers, decision-makers, and stakeholders requiring de-

tailed information on land surface states. Further details on ERA5-Land can be found in (Muñoz-Sabater et al., 2021). Spatial distribution of selected stations and corresponding grids of ERA5-Land is shown in Figure 2.4.

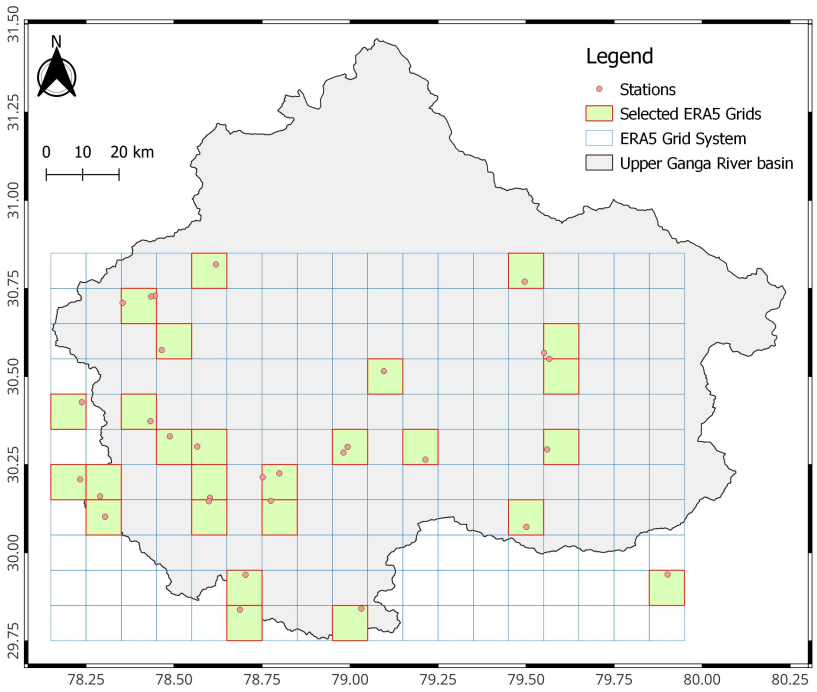

Figure 2.4: Distribution of ERA5-Land grids and selected stations in UGB.

IMDAA: Indian Monsoon Data Assimilation and Analysis

IMDAA is a regional atmospheric reanalysis, developed through a collaborative effort between the National Centre for Medium Range Weather Forecasting (NCMRWF), India, and the United Kingdom's Met Office (UKMO). This initiative, conducted in collaboration with the India Meteorological Department (IMD) under the National Monsoon Mission (NMM) project, spearheaded by the Ministry of Earth Sciences, Government of India, seeks to produce a high-resolution reanalysis for South Asia and adjacent regions. IMDAA leverages advanced data assimilation techniques and numerical weather prediction (NWP) systems, providing datasets with a horizontal resolution of 12 km ($0.12° \times 0.12°$). The reanalysis spans the satellite era, covering the period from 1979 to the present. The IMDAA assimilation system integrates both satellite-derived and conventional obser-

vational data within a 6-hour assimilation window (Rani et al., 2021; Singh et al., 2021). Spatial distribution of selected stations and corresponding grids of IMDAA is shown in Figure 2.5.

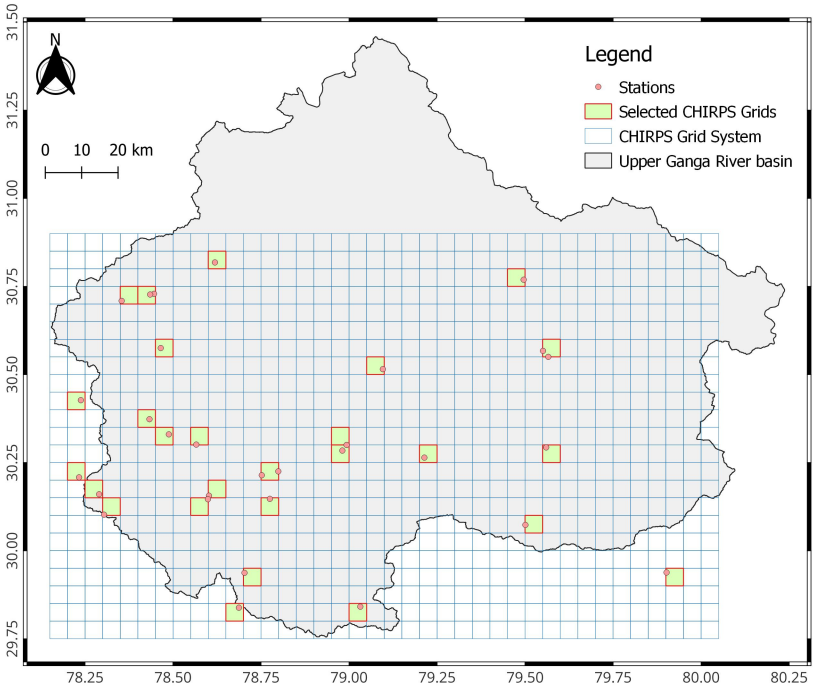

Figure 2.5: Distribution of IMDAA grids and selected stations in UGB.

2.2.2.3 Station Derived Gridded Observation

IMD Observed Gridded Precipitation

India Meteorological Department (IMD) provides high resolution 25 km (0.25° x 0.25°) gridded precipitation product. This product is available for the longer time period starting from the year 1901 to present day over the mainland India and have been used widely in research focusing on climatology (Bisht et al., 2018, 2019; Meher et al., 2017) satellite rainfall evaluation (Banerjee et al., 2020; Beria et al., 2017). The IMD gridded product is developed using daily rainfall records from 6995 rain gauge stations across the country after quality control (Pai et al., 2014). However, these numbers varies from year to year based on the number

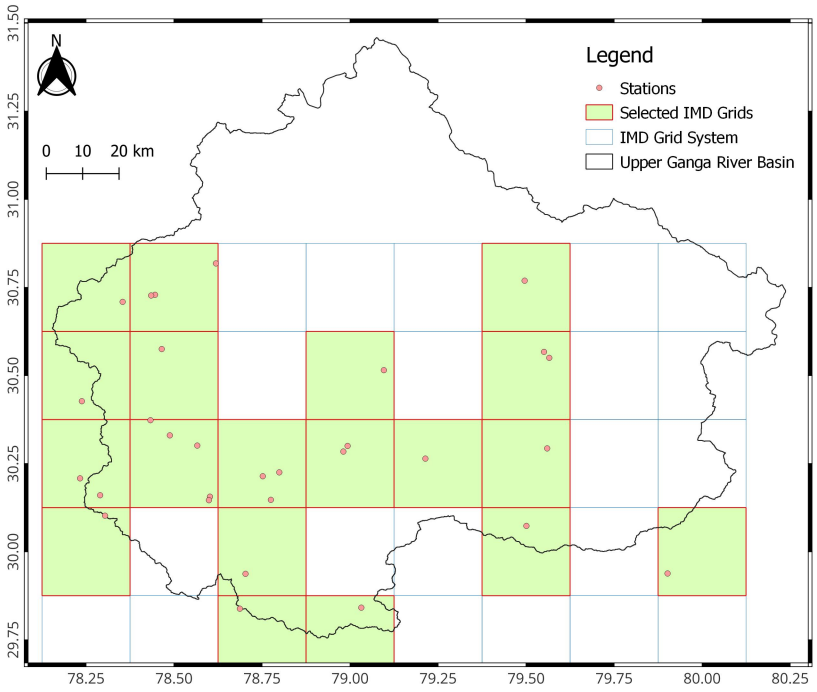

Figure 2.6: Distribution of IMD grids and selected stations in UGB.

of operational rain gauge station. In Himalayas, there is undulating topography, and paucity of ground based observatory (rain-gauge and radar network) are very sparse to get accurate measurements of rainfall information. In particular, it is important to mention the deficit of observatories beyond 2000 m affects the overall quality of precipitation estimates at high altitude region. Spatial distribution of selected stations and corresponding grids of IMD gridded precipitation dataset is shown in Figure 2.6.

Chapter 3

Methodology

Precipitation Estimates (PEs) from various datasets can be evaluated using suitable statistical techniques for their efficacy vis-a-vis specific region. However, besides providing the statistical evaluation, it is also crucial to perform the ranking of these products while considering different statistical criterion to gain more insight regarding their utility. This calls for the need of multicriterion decision-making (MCDM) approach to incorporate different statistical attributes of these PEs and Group decision-making (GDM) approaches to obtain their overall ranking based on their performance.

In subsequent sections detail about performance indicators, MCDM and GDM based ranking approaches are discuss in detail.

3.1 Performance indicator

To evaluate the ability of global climatological data in resolving the regional or local scale climatology, appropriate performance indicators should be utilized. In the context of present study, the performance indicator is a measure of any global precipitation estimate in capturing the behaviour of precipitation as produced by observed gridded record. Pearson correlation coefficient (CC), Percentage bias

(PBIAS), Probability of detection (POD), False alarm ratio (FAR), Nash–Sutcliffe efficiency (NSE), Root mean square error (RMSE), Skill score (SS), Mean Absolute Error (MAE), Relative bias (RBIAS) are some of the commonly employed performance indicator to evaluate the satellite rainfall vis-a-vis observed records (Beria et al., 2017; Chowdhury et al., 2021; Shukla et al., 2019).

Chowdhury et al. (2021) reported that no specific evidence are available in favour of any specific performance indicators therefore, based on the users' discretion appropriate indicators can be chosen for evaluation. Therefore, apart from using POD and FAR, three other performance indicators, viz., Normalised Root Mean Squared dviation (NRMSD), Pearson's Correlation Coefficient (CC) and Skill Score (SS) were employed (Table 3.1) for skill evaluation and performance ranking of PE following Srinivasa Raju & Nagesh Kumar (2015a). These three indicators, i.e., NRMSD, CC, and SS are easy to interpret and appropriate for such evaluations and represent the difference, strength of linear association, and similarity between the probability distribution function of reference and targeted time series, respectively. These three indicators were employed in MCDM analysis, which is discussed in detail in section 3.2.3.

Table 3.1: Summary of performance indicators used to evaluate the PEs

Indicator	Mathematical expression	Range	Remark
NRMSD	$\frac{\sqrt{\frac{1}{N}\sum_{i=1}^{N}(obs_i - mod_i)^2}}{\overline{obs}}$	$\in [0\ ,\ \infty)$	Smaller value is favourable.
CC	$\frac{\sum_{i=1}^{N}\left(obs_i - \overline{obs}\right)\left(mod_i - \overline{mod}\right)}{(N-1)\sigma_{obs}\sigma_{mod}}$	$\in$ [-1,1]	Best value is 1, worst value is -1
SS	$\frac{1}{N}\sum_{i=1}^{nb}\min\left(f_{mod}f_{obs}\right)$	$\in$ [0,1]	Best value is 1, worst value is 0

N is the length of dataset.
obs_i and mod_i are the observation and modeled (Precipitation Estimates, in present context) values, respectively.
$\overline{obs}$ and $\overline{mod}$ are the mean of observed and modeled values, respectively.
σ_{obs} and σ_{mod} are the standard deviation of observed and modeled values, respectively.
nb is the number of bins for calculating the probability density function for specific grid or region, and f_{mod} and f_{obs} are the frequencies of values in a specific bin from the modeled and observed dataset, respectively.

3.2 Application of MCDM and GDM for performance ranking

Multicriterion Decision-Making (MCDM) aids in analysing complex problems that involves different evaluation criterion and multiple alternatives. The MCDM approach is used in present study as multiple alternatives (i.e., PEs) were compared for their performance based on different criterion i.e., performance indicators. Out of five performance indicators shown in Table 3.1, NRMSD, CC, and SS were used to rank each PE based on different MCDM approaches explained in section 3.2.3 and 3.2.4.

Normalization of indicators and weight determination for different criterion is required as different indicators might target different attributes and represent conflicting criteria. Different normalization techniques used in this report are presented in section 3.2.1. Relative importance or weight determination for different criterion is briefly discussed in section 3.2.2.

In the presence of multiple decision-makers, it becomes imperative to integrate the outcome of each decision-makers to obtain the final results. Group decision-making (GDM) helps in integrating the multiple decision-making criterion by analysing rank correlation and suitable rank combining rules. Section 3.2.5 briefly discuss the GDM approach used in this study. A methodology flowchart of application of MCDM and GDM is provided in Figure 3.1.

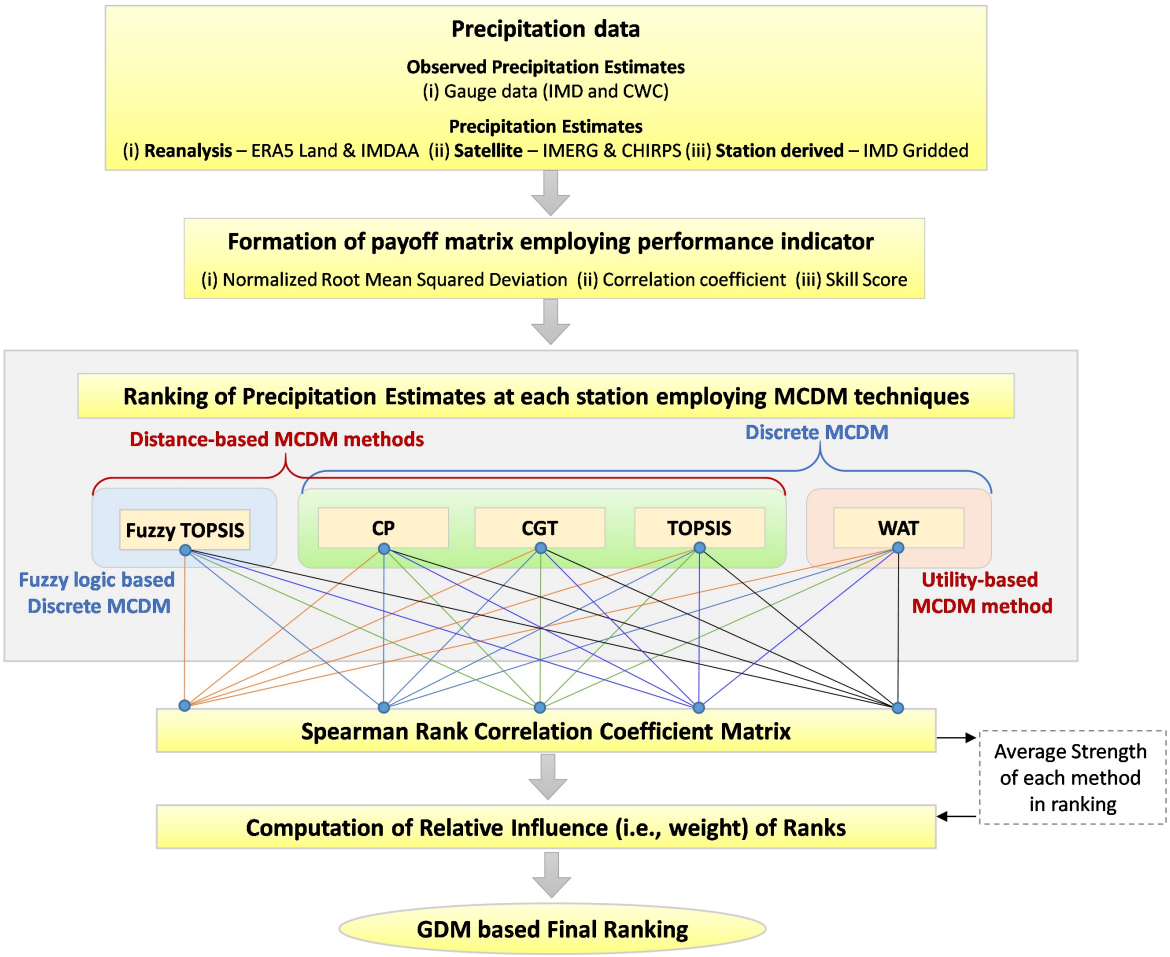

Figure 3.1: Flowchart of MCDM and GDM based PE ranking

3.2.1 Normalization Techniques

Ranges of different performance indicators vary in different space and often cannot be compared with each other without applying appropriate statistical operation to restrict them within same space. For example, NRMSD may take any value between 0 and ∞, whereas the SS is limited to 0 and 1. Besides, depending upon the nature of datasets the values of these indicators might clustered differently. Details of different normalization techniques can be referred in Pomerol & Barba-Romero (2000).

In this study, two types of normalization techniques, which can be termed as Norm-1 (eq. 3.1) and Norm-2 (eq. 3.2) for ease of conveying, have been employed.

$$v_i = \frac{x_i}{\sum_i^N x_i} \tag{3.1}$$

$$v_i = \frac{x_i - \min x_i}{\max x_i - \min x_i} \tag{3.2}$$

Where, v_i is the normalized vector, x_i is the value of indicator, N is the number of alternatives (i.e., PEs in the context of present study). Normalized vector obtained using Norm-1 technique ($\in$ (0,1)) conserve the proportionality unlike Norm-2 technique ($\in$ [0,1]).

3.2.2 Weight determination using Entropy technique

In MCDM analysis, it is imperative to consider all the decision makers (i.e., performance indicators in the context of present study) to reach the final outcome. However, as different decision makers evaluate the alternative for their specific skill it is essential to assign appropriate weight or relative importance to each decision maker. There are different methods available for weight determination which can be referred in Pomerol & Barba-Romero (2000). However, in present study Entropy method was used for weight determination following Srinivasa Raju & Nagesh Kumar (2015a) and Chowdhury et al. (2021).

Though detailed description of entropy based weight determination is provided in Pomerol & Barba-Romero (2000), steps of Entropy method are explained herein for ease of understanding.

Step 1: Create the normalized payoff matrix employing Norm-1 technique (eq. 3.1) for all the decision makers (i.e., performance indicators).

Step 2: Compute entropy for each decision maker as follows,

$$En_j = -\frac{1}{\ln(N)} \sum_{i=1}^{N} v_{ij} \ln(v_{ij}) \qquad \text{for } j = 1, \ldots, J \tag{3.3}$$

Where, En_j is the entropy for each decision maker (i.e., performance indicator or criterion), N is the number of alternatives (i.e., PEs), i is the index of alternative, v_{ij} is the normalized value for i_{th} alternative and j_{th} decision maker.

Step 3: Compute degree of diversification D_j for each decision maker,

$$D_j = 1 - En_j \qquad \text{for } j = 1, \ldots, J \tag{3.4}$$

Step 4: Normalize the weights employing Norm-1 technique (eq. 3.1,

$$w_j = \frac{D_j}{\sum_{j=1}^{J} D_j} \tag{3.5}$$

Higher entropy value (eq. 3.3) represents higher degree of uncertainty associated with the criterion, which results into smaller degree of diversification (eq. 3.4) making the criterion less important by assigning smaller weight (eq. 3.5).

Weight determined using entropy methods were used in MCDM analysis for carrying-out performance ranking of selected PEs as discussed in section 3.2.3 and 3.2.4.

3.2.3 Discrete Multicriterion Decision Making in deterministic scenario

In literature, there are different types of discrete MCDM analysis approaches are available in deterministic scenario. In present study, two types of Discrete MCDM methods in deterministic scenario have been employed , (i) Distance based method,

and (ii) Utility based method.

Among distance based method, Compromise Programming (section 3.2.3.1), Cooperative Game Theory (section 3.2.3.2), and Technique for Order Preference by Similarity to an Ideal Solution (section 3.2.3.3) have been used. Weighted Average Technique (section 3.2.3.4) is used from various available Utility based methods.

Here it should be noted that rational of employing multiple MCDM methods for rank determination is to eventually use group decision making approach to obtain final ranking that will not only have multiple decision makers but also varying computation methods.

3.2.3.1 Compromise Programming (CP)

This methods aims to obtain the best solution which has the least distance from the ideal solution (Srinivasa Raju et al., 2017). The distance measure for finding the best solution is represented by $L_p - metric$. Steps to perform MCDM based ranking employing Compromise Programming are as follows,

Step 1: Create the normalized payoff matrix employing Norm-1 technique (eq. 3.1) for all the decision makers for weight computation.

Step 2: Find ideal value for each decision maker j among available alternatives, i.e., for CC and NRMSD, highest and lowest value, respectively, among all the alternatives would be the ideal values.

Step 3: Compute the $L_p - metric$ for each alternative as follows,

$$L_{pi} = \left[\sum_{j=1}^{J} w_j^p \left| x_j^* - x_{ji} \right|^p \right]^{\frac{1}{p}} \qquad \text{for } i = 1, \ldots, N \tag{3.6}$$

Where, L_{pi} is the $L_p - metric$ for i_{th} alternative, w_j is the weight assigned to decision maker j, x_j^* is the ideal value for j_{th} decision maker, x_{ji} is the value

of j_{th} decision maker for i_{th} alternative, N is the number of alternatives, and p is the parameter for distance metric. Following Chowdhury et al. (2021) Euclidean distance is considered by taking $p = 2$.

Step 4: Find the ranking of suitable alternative from estimated L_{pi} values. Most suitable alternative will have lowest L_{pi} and vice-versa.

3.2.3.2 Cooperative Game Theory (CGT)

In this method, unlike Compromise Programming, the best solution is one which has farthest distance from the anti-ideal solution rather than the least distance from the ideal solution (Gershon & Duckstein, 1983). Cooperative Game Theory uses geometric distance measure to obtain the ranking of various alternatives. Steps to perform MCDM based ranking employing CGT approach are as follows,

Step 1: Create the normalized payoff matrix employing Norm-1 technique (eq. 3.1) for all the decision makers for weight computation.

Step 2: Find anti-ideal value for each decision maker j among available alternatives, i.e., for CC and NRMSD, lowest and highest value, respectively, among all the alternatives would be the anti-ideal values.

Step 3: Compute the geometric distance (G) for each alternative as follows,

$$G_i = \prod_{j=1}^{J} \left| x_{ji} - x_j^{**} \right|^{w_j} \qquad \text{for } i = 1, \ldots, N \tag{3.7}$$

Where, G_i is the geometric distance for i_{th} alternative, w_j is the weight assigned to decision maker j, x_j^{**} is the anti-ideal value for j_{th} decision maker, x_{ji} is the value of j_{th} decision maker for i_{th} alternative, and N is the number of alternatives.

Step 4: Find the ranking of suitable alternative from estimated G_i values.

Most suitable alternative will have highest G_i value and vice-versa.

3.2.3.3 Technique for Order Preference by Similarity to an Ideal Solution (TOPSIS)

This method aims to find the best solution considering the least distance from the ideal solution like compromise programming as well as the farthest distance from the anti-ideal solution like cooperative game theory (Opricovic & Tzeng, 2004). Steps to perform MCDM based ranking employing TOPSIS method are as follows,

Step 1: Create the normalized payoff matrix employing Norm-1 technique (eq. 3.1) for all the decision makers for weight computation.

Step 2: Find the ideal (v_i) and anti-ideal (v_{ai}) value for each decision maker as explained in sections 3.2.3.1 and 3.2.3.2, respectively.

Step 3: Compute the separation measure (Opricovic & Tzeng, 2004; Srinivasa Raju & Nagesh Kumar, 2015b) of each alternative (i.e., distance) from the ideal and anti-ideal solution, and relative closeness of alternative from ideal solution as follows,

$$DS_i^+ = \sqrt{\sum_{j=1}^{J} \left(w_j x_{ji} - w_j x_j^*\right)^2} \qquad \text{for } i = 1, \ldots, N \tag{3.8}$$

$$DS_i^- = \sqrt{\sum_{j=1}^{J} \left(w_j x_{ji} - w_j x_j^{**}\right)^2} \qquad \text{for} i = 1, \ldots, N \tag{3.9}$$

$$CR_i = \frac{DS_i^-}{DS_i^- + DS_i^+} \qquad \text{for} i = 1, \ldots, N \tag{3.10}$$

Where, DS_i^+ and DS_i^- are the separation measure from the ideal and

anti-ideal solutions for i_{th} alternative, respectively; w_j is the weight assigned to decision maker j; x_j^* and x_j^{**} are the ideal and anti-ideal value for j_{th} decision maker, respectively; x_{ji} is the value of j_{th} decision maker for i_{th} alternative; N is the number of alternatives; and CR_i is the relative closeness of i_{th} alternative from the ideal solution.

Step 4: Find the ranking of suitable alternative from estimated CR_i values. Most suitable alternative will have highest CR_i value and vice-versa.

3.2.3.4 Weighted Average Technique (WAT)

Unlike, CP, CGT, and TOPSIS approaches of MCDM, Weighted Average Technique is a utility based method. In this method, utility of each alternative is computed for assigning performance ranking. Steps to perform MCDM based ranking employing WAT method are as follows,

Step 1: Create the normalized payoff matrix employing Norm-1 technique (eq. 3.1) for all the decision makers for weight computation.

Step 2: Compute the utility (U) of each alternative as follows,

$$U_i = \sum_{j=1}^{J} w_j xj \qquad \text{for } i = 1, \ldots, N \tag{3.11}$$

Where, U_i is the utility of i_{th} alternative, w_j is the weight assigned to decision maker j, x_j is the value of j_{th} decision maker for i_{th} alternative, and N is the number of alternatives.

Step 4: Find the ranking of suitable alternative from estimated U_i values. Most suitable alternative will have highest U_i value and vice-versa.

3.2.4 Discrete Multicriterion Decision Making in fuzzy scenario

In MCDM analysis uncertainty can arise during to weight assessment of the criteria or during evaluating the alternatives with respect to specific criteria (Srinivasa Raju & Nagesh Kumar, 2010). This uncertainty can be addressed in the fuzzy scenario wherein the relative values of attributes were assigned using fuzzy numbers to perform the MCDM analysis. In this study, fuzzy TOPSIS method was employed following Bisht et al. (2024), Chowdhury et al. (2021) and Srinivasa Raju & Nagesh Kumar (2015a). Fuzzy TOPSIS method employed in this study is explained in detail in section 3.2.4.1.

3.2.4.1 Fuzzy Technique for Order Preference by Similarity to an Ideal Solution (Fuzzy TOPSIS)

The Fuzzy TPOSIS method of MCDM works on the same principle as explained in TOPSIS (section 3.2.3.3), i.e., best solution should have least distance from the ideal solution and farthest distance from the anti-ideal solution. However, unlike TOPSIS, in Fuzzy TOPSIS the distance estimation is carried out through fuzzy logic (Yang & Hung, 2007). In this study triangular membership function (TMF) was utilized for fuzzification following Bisht et al. (2024), Chowdhury et al. (2021), Srinivasa Raju & Nagesh Kumar (2015a) and Yang & Hung (2007) due to its simplistic nature and ease of interpretation.

A fuzzy number $\tilde{A}$ with triangular membership function is characterized by (a_1, a_2, a_3), $a_1 \prec a_2 \prec a_3$ as shown in Figure 3.2. Mathematical expression for TMF is presented in equation 3.14.

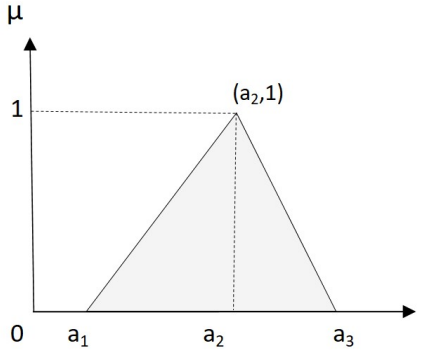

Figure 3.2: Triangular membership function for fuzzy number Ã

$$\mu_{\tilde{A}}(x) = \begin{cases} 0, & x \leqslant a_1 \\ \frac{x-a_1}{a_2-a_1}, & a_1 < x \leqslant a_2, \\ \frac{a_3-x}{a_3-a_2}, & a_2 < x \leqslant a_3, \\ 0, & x > a_3 \end{cases} \tag{3.12}$$

The distance $d(\tilde{A}, \tilde{B})$ between two fuzzy numbers $\tilde{A} = (a_1, a_2, a_3)$ and $\tilde{B} = (b_1, b_2, b_3)$ is calculated as,

$$d(\tilde{A}, \tilde{B}) = \sqrt{\frac{1}{3}\left[(a_1 - b_1)^2 + (a_2 - b_2)^2 + (a_3 - b_3)^2\right]} \tag{3.13}$$

The basic arithmetic operations between two fuzzy numbers $\tilde{A} = (a_1, a_2, a_3)$ and $\tilde{B} = (b_1, b_2, b_3)$ are as follows,

$$\tilde{A} + \tilde{B} = (a_1 + b_1,\ \ a_2 + b_2,\ \ a_3 + b_3)$$

$$\tilde{A} - \tilde{B} = (a_1 + b_3,\ \ a_2 - b_2,\ \ a_3 + b_1)$$

$$\tilde{A} \times \tilde{B} = (a_1 b_1,\ \ a_2 b_2,\ \ a_3 b_3)$$

$$\tilde{A} \div \tilde{B} = (a_1/b_3,\ \ a_2/b_2,\ \ a_3/b_1)$$

In the present study, five-level linguistic variables were used to obtain the ranking through fuzzy logic in Fuzzy TOPSIS. To assign these linguistic variable to precise values following scheme (Table 3.2, Figure 3.3) of Yang & Hung (2007) was utilized,

Table 3.2: Linguistic variables used in triangular fuzzy membership function

Rank	Membership Function
Very Low (VL)	(0.00, 0.10, 0.25)
Low (L)	(0.15, 0.30, 0.45)
Medium (M)	(0.35, 0.50, 0.65)
High (H)	(0.55, 0.70, 0.85)
Very High (VH)	(0.75, 0.90, 1.00)

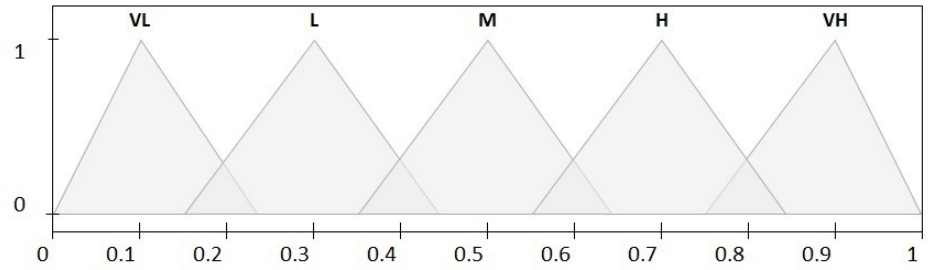

Figure 3.3: Scheme of fuzzy triangular membership scheme

$$\mu_{\tilde{A}}(x) = \begin{cases} 0, & x \leqslant a_1 \\ \frac{x-a_1}{a_2-a_1}, & a_1 < x \leqslant a_2, \\ \frac{a_3-x}{a_3-a_2}, & a_2 < x \leqslant a_3, \\ 0, & x > a_3 \end{cases} \tag{3.14}$$

Performance ranking of various alternatives using Fuzzy TOPSIS in MCDM approach can be obtained in following steps,

Step 1: Create the normalized payoff matrix employing Norm-1 technique (eq. 3.1) for all the decision makers for weight computation.

Step 2: Create the normalized payoff matrix employing Norm-2 technique (eq. 3.2) to create normalized payoff matrix to utilize in fuzzy logic. Here, Norm-2 technique is used as it provides wider range ($\in [0, 1]$) unlike Norm-1 technique which is clustered in a comparatively small range ($\in (0, 1)$). The wider range helps in utilizing all the Linguistic variables in fuzzy logic as presented in Table 3.2.

Step 3: Utilizing the triangular membership function (eq. 3.14) and Table 3.2, transform the payoff matrix (Table 3.3) into fuzzy linguistic variables (Table 3.4), as follows .

Table 3.3: Normalized payoff matrix example for Fuzzy TOPSIS analysis

	DM1	**DM2**	**DM3**
A1	0.70	0.60	0.12
A2	0.10	0.18	0.71
⋮	⋮	⋮	⋮
An	0.49	0.80	0.46
w	0.30	0.50	0.20

Table 3.4: Payoff matrix example using linguistic variables

	DM1	**DM2**	**DM3**
A1	H	M	VL
A2	VL	VL	H
⋮	⋮	⋮	⋮
An	M	H	M
w	L	M	L

Step 4: Transform Table 3.4 into fuzzy-weighted decision matrix by assigning corresponding triangular membership function to Linguistic variables in Table 3.4 from Table 3.2 and multiplying the weight (w) with each membership function.

Step 5: Compute the separation measure DS_i^+ and DS_i^- (Srinivasa Raju & Nagesh Kumar, 2010; Yang & Hung, 2007) of each alternative (i.e., distance) from the ideal, $\tilde{Y}^* = (y_1^*, y_2^*, y_3^*)$, and anti-ideal, $\tilde{Y}^{**} = (y_1^{**}, y_2^{**}, y_3^{**})$, solution following eq. 3.13. Here, ideal and anti-ideal values are $\tilde{v}_i = (1, 1, 1)$ and $\tilde{v}_{ai} = (0, 0, 0)$, respectively.

Step 6: Compute the relative closeness CR_i of alternative from ideal solution using eq. 3.10.

Step 7: Find the ranking of suitable alternative from estimated CR_i values. Most suitable alternative will have highest CR_i value and vice-versa.

3.2.5 Group Decision Making

In group decision making approach, the ranking provided by different ranking approaches are integrated to obtain the most acceptable ranking rather than relying on the results of one single method which might have its own limitations or advantages (Morais & de Almeida, 2012).

In this study, the group decision making was performed to collate the rankings provided by all the five used MCDM methods (i.e., CP, CGT, TOPSIS, WAT, and Fuzzy TOPSIS) over each grid into single representative ranks. Spearman rank correlation (Bisht et al., 2024; Chowdhury et al., 2021) was used to find the average strength of each MCDM method (Srinivasa Raju & Nagesh Kumar, 2010) of each MCDM method. These average strengths were normalized using Norm-1 technique (eq. 3.1) for weight assignment to respective MCDM method for integrating the ranks.

3.2.5.1 Spearman rank correlation

The association between the ranks obtained using different MCDM methods can be assesed by Spearman rank correlation (ρ). If K_1 nd K_2 are the two different ranks of an alternative A_1 using two different approaches, then following Gibbons & Chakraborti (2014), ρ can be expressed as,

$$\rho = 1 - \frac{6 \sum_{a=1}^{N} D_{A1}^2}{N\left(N^2 - 1\right)} \tag{3.15}$$

Where, D_{A1} is the difference between ranks i.e., $(K_1 - K_2)$, for the same alternative A_1, and N is the number of alternatives.

An example of average strength computation is presented in Table 3.5; ρ values ≤ 2 as and diagonal values are not considered in the computation as presented in the highlighted cell. Rank correlation classification provided by Connolly & Sluckin (1971) is presented in Table 3.6.

Table 3.5: Computation of average strength of each MCDM method using Spearman rank correlation coefficient

MCDM method	M1	M2	M3	M4	M5	Sum	Number of considered element	Average Strength
M1	⋱	0.94	0.88	0.31	0.48	2.61	4	0.65
M2	0.94	⋱	0.94	0.16	0.25	2.13	3	0.71
M3	0.88	0.94	⋱	0.19	0.73	2.55	3	0.85
M4	0.31	0.16	0.19	⋱	0.90	1.21	2	0.61
M5	0.48	0.25	0.73	0.90	⋱	2.36	4	0.59

(Average strength is estimated by dividing the sum of considered ρ values from number of considered elements.)

Table 3.6: Rank correlation classification

ρ value	Nature of relationship
0.9-1.0	Very strong
0.7-0.9	Marked
0.4-0.7	Substantial
0.2-0.4	Definite
≤ 0.2	Small (can be neglected)

3.2.5.2 Additive ranking rule

After computation of average strength of each MCDM method, the final representative rank of each alternative at each grid is computed using additive ranking rule (Srinivasa Raju & Nagesh Kumar, 2010) as follows,

$$R_A^M = \frac{\sum_{m=1}^{M} w_m K_A^m}{M} \tag{3.16}$$

Where, R_A^M is the final rank of each alternative after integrating all the ranks of that alternative obtained by M number of MCDM methods; w_m is the weight or relative influence of each MCDM method; and K_A^m is the rank obtained by each alternative using each MCDM method m.

Chapter 4

Results and Discussion

Four fine-resolution Precipitation Estimates (PEs) were selected for analysis: two from Satellite Precipitation Estimates (SPEs) and two from Reanalysis Precipitation Estimates (RPEs), along with one station-derived gridded precipitation estimate from the India Meteorological Department (IMD) which has been widely used as a reference dataset over India. A detailed description of these products is provided in Chapter 2. The study covers 18 hydrological years, from June 1, 2000, to May 31, 2018, during which the selected PEs were analyzed and ranked categorically using Multi-Criteria Decision Making (MCDM) and Groud Decision Making (GDM) techniques, as discussed in Chapter 3. The PEs were evaluated for each grid with respect to corresponding station(s) falling within that grid. If a specific grid contained more than one station, the PE for that grid was evaluated for both stations (refer to the maps of PE grids and station distribution in Chapter 2). This approach accounts for the spatial variability of precipitation in localized systems which is often reflected in stations situated in close proximity.

4.1 Evaluation of PEs in reproducing regional precipitation cycle

The skill of the PEs in resolving the precipitation climatology of the region, in comparison to the station observation, was assessed using graphical methods. Regional precipitation cycle derived from each PE was compared with station records for 18 hydrological years i.e., June 2000 - May 2018 (Figure 4.1) for yearwise (Figure 4.1a,d,g,i,and m) and for entire 18 years of duration (Figure 4.1b,e,h,k, andn). To analyze the yearwise regional precipitation cycle, the areal monthly precipitation was computed for each month by including all stations and their corresponding grids for each respective PE. For the overall precipitation climatology over the entire study period, the mean monthly areal precipitation for the Upper Ganga Basin (UGB) was calculated by considering the monthly precipitation data from all selected stations and their corresponding grids for each respective PE. Furthermore, the comparative analysis was also performed for monthly areal precipitation across all the years to find the linear association between various PEs and IMD precipitation (Figure 4.1 c,f,i,l, and o).

The analysis reveals a consistent overestimation by IMDAA, a Reanalysis Precipitation Estimate (RPE), throughout the study period (Figure 4.1g), which is also evident in the scatter plot (Figure 4.1i) and overall precipitation climatology (Figure 4.1h). The significant overestimation by IMDAA is particularly noticeable. In contrast, ERA5-Land, another RPE, demonstrates a more reasonable accuracy in capturing the precipitation cycle, with better performance than IMDAA (Figure 4.1a, b, and c). Among the Satellite Precipitation Estimates (SPEs), IMERG accurately captures the precipitation cycle and shows good agreement with station-derived precipitation data (Figure 4.1d,e, and f). Notably, CHIRPS, another RPE, consistently underestimated precipitation during the initial phase from 2000 to 2010 (Figure 4.1j). However, it captures the precipitation climatology with reasonable accuracy after 2010. The underestimation by CHIRPS in the initial phase affects the overall resolution of the precipitation climatology derived from it, leading to an underestimation of the precipitation cycle in the Upper Ganga Basin (UGB) (Figures 4.1k and l).

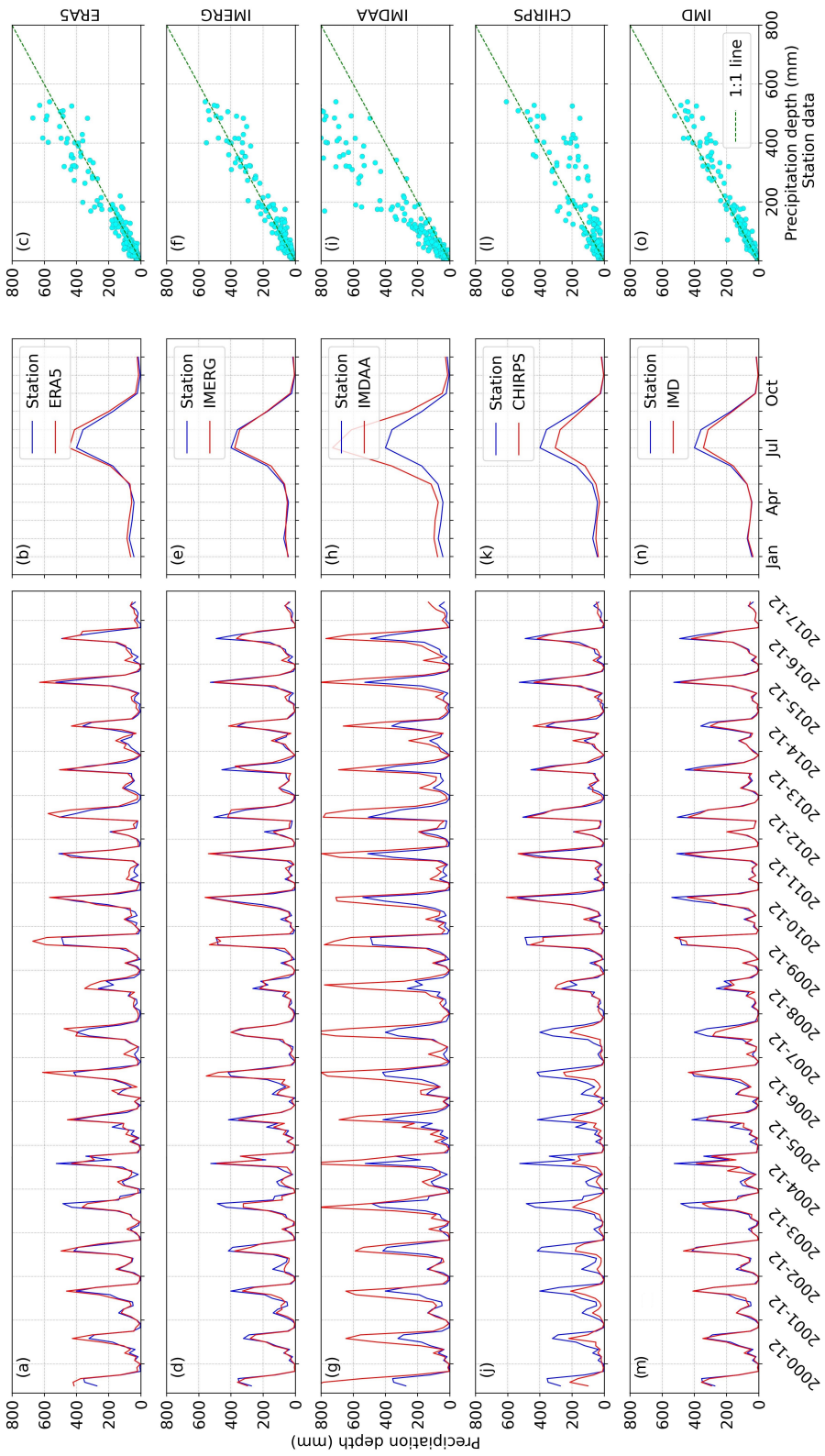

Figure 4.1: Comparison of regional precipitation of selected PEs with station records.

The IMD gridded dataset, derived from station records, exhibits good accuracy in resolving the precipitation climatology (Figures 4.1n and o), though it occasionally overestimates regional rainfall in some years (Figure 4.1m).

From the analysis presented in Figure 4.1, a general inference can be drawn regarding the overall skill of these products in resolving the precipitation climatology. IMERG, ERA5, and the IMD gridded products emerge as better-suited alternatives over CHIRPS ad IMDAA for the UGB. However, it is important to note that the IMD gridded product is developed using station data; hence, its performance may be compromised in areas with sparse station coverage. In such regions, where station records are of poor quality or unavailable, IMERG and ERA5 can be recommended as more reliable precipitation datasets for evaluation and analysis. Further efforts were made to rank these precipitation products using Multi-Criteria Decision-Making (MCDM) and Group Decision-Making (GDM) techniques at each station. Performance ranking was conducted for precipitation time series at daily scale, monthly scale, and monthwise scale.

4.2 Performance ranking of PEs using MCDM methods

To determine the categorical ranking of the PEs i.e., IMERGE, CHIRPS, ERA5-Land, IMDAA, and IMD gridded datasets were evaluated for their performance employing three performance indicators namely, NRMSE, CC, and SS (Table 3.1). Performance ranking was determined considering the data for common period, i.e., Jun 2000 to May 2018, during which precipitation is available for all the five PEs. Common period is selected to avoid the ambiguity in final results that might arise due to varying period of dataset. As illustrated in Figure 3.1) and explained in section 3.2, a total of five different MCDM techniques i.e., CP, CGT, TOPSIS, WAT, and Fuzzy TOPSIS were employed to obtain the performance rank of each PE for all the identified grids. Ranking of PEs were obtained for daily time series (section 4.2.1), monthly time series (section 4.2.2), and monthwise time series

(section 4.2.3) as discussed ahead.

4.2.1 MCDM based performance ranking using daily time series

Daily time series were analyzed to rank the performance of selected Precipitation Estimates (PEs) using various Multi-Criteria Decision Making (MCDM) methods, as detailed in Chapter 3. A heatmap of performance indicators, namely Normalized Root Mean Square Deviation (NRMSD), Correlation Coefficient (CC), and Skill Score (SS), is presented in Figure 4.5. The IMD gridded dataset (hereafter IMD) and ERA5-Land (hereafter ERA5) exhibit smaller NRMSD and higher CC (Figure 4.5) compared to IMDAA, CHIRPS, and IMERG for the majority of stations. IMERG, CHIRPS, and IMD generally show better SS across most stations. However, it's important to note that SS shows very small variation, making the differences between the PEs statistically insignificant. Therefore, to derive meaningful conclusions from these indices, it is essential to apply an MCDM technique to integrate these indicators, leading to an objective assessment of the suitability of these PEs.

To suitably utilize the strength and limitation of these performance indicators, their weights were determined using entropy technique for each station as explained in section 3.2.2. As presented in Figure 4.3, NRMSD and SS show higher entropy values in the range $\in (0.9, 1)$ in comparison to CC. This infers that contrary to CC, NRMSD and SS have large uncertainty associated with them. Since the CC showed lesser entropy in comparison to NRMSD and SS, it was assigned higher weight (eq. 3.4 and eq. 3.5) as shown in Figure 4.3. Also, NRMSD was assigned higher weights in comparison to SS, as it showed relatively smaller entropy.

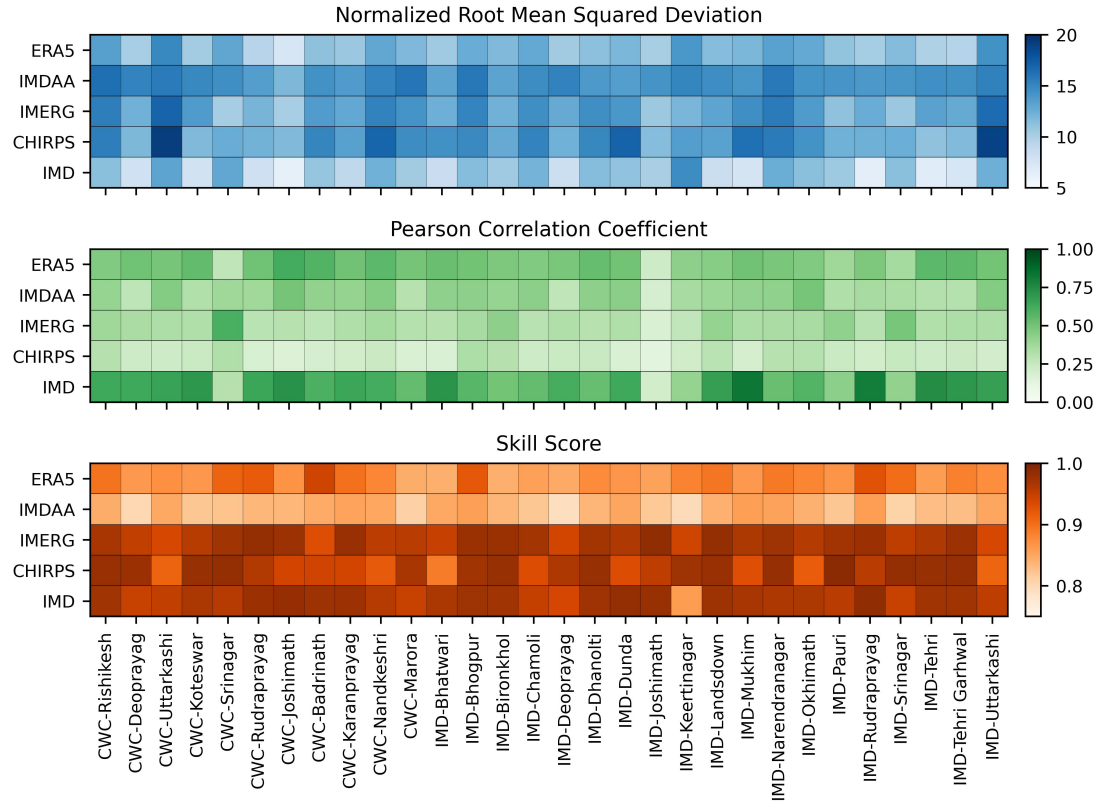

Figure 4.2: Performance indicator for daily time series.

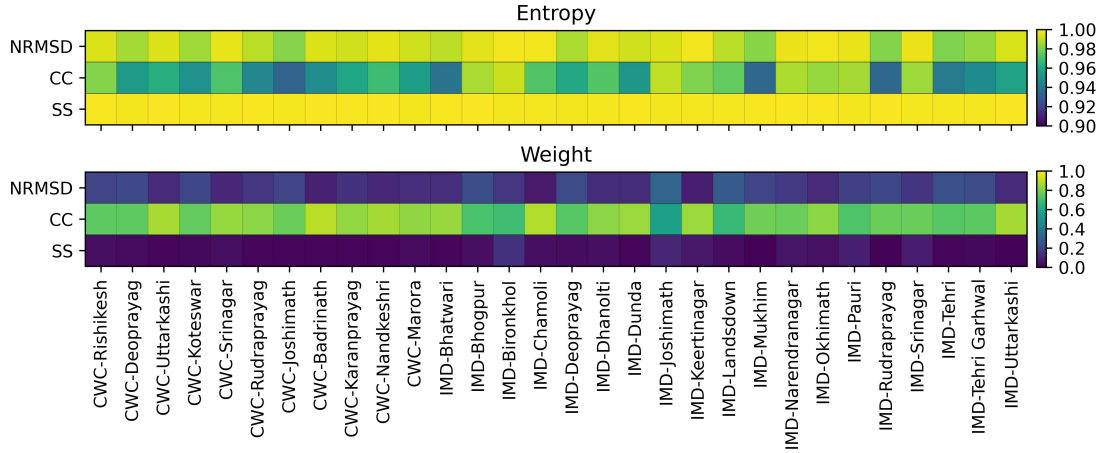

Figure 4.3: Entropy value and weight assigned to performance indicators for computing performance ranking employing daily time series.

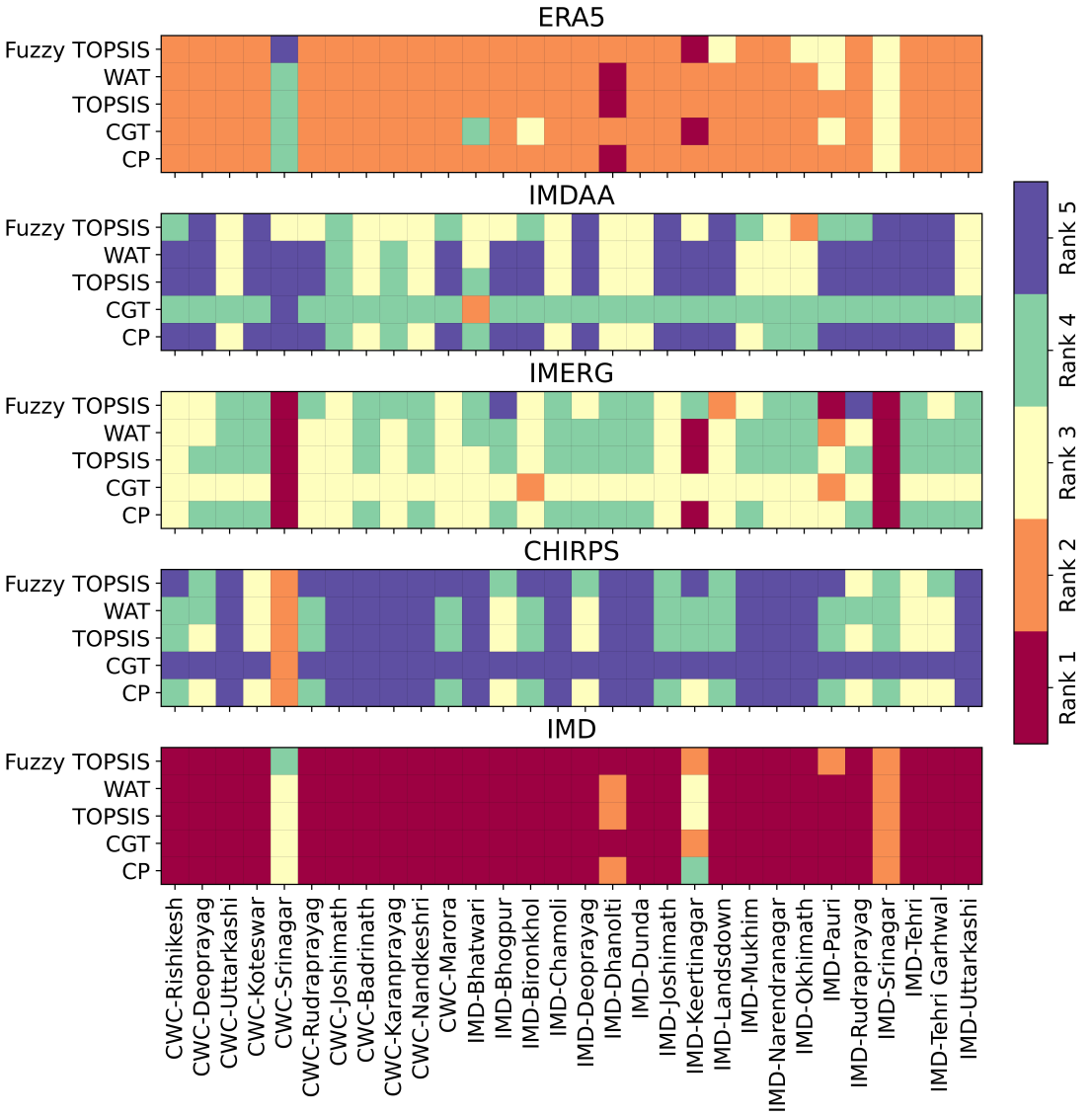

Figure 4.4: Performance ranking of PEs employing daily time series and different MCDM techniques.

Using the weights derived from the entropy technique, the performance rankings of PEs were determined for each station, as shown in Figure 4.4. It is evident that, with the exception of IMD and ERA5—which were predominantly ranked first and second, respectively—the remaining PEs were assigned varying ranks by different Multi-Criteria Decision Making (MCDM) methods across most stations. As evident from the Figure 4.4 IMDAA and CHIPRS were ranked max-

imum number of times at several stations. While IMD is clearly identified as the best-performing PE, consistently ranked first by all MCDM techniques for the majority of stations, ERA5 is similarly ranked second by these methods. However, it is challenging to assign a specific rank to the other PEs, namely IMERG, CHIRPS, and IMDAA, as they received different rankings across a significant number of stations depending on the MCDM method used. Consequently, it is essential to consolidate the ranks obtained from the different MCDM methods into a single representative rank. This integration is achieved through the Group Decision Making (GDM), as detailed in Section 3.2.5, and the results are presented in section 4.3.

4.2.2 MCDM based performance ranking using monthly time series

The monthly time series were analyzed following the similar approach to that used for the daily time series. To facilitate this analysis, the daily data were first aggregated into monthly time series for both the stations and the corresponding grid points. A heatmap of performance indicators, namely Normalized Root Mean Square Deviation (NRMSD), Correlation Coefficient (CC), and Skill Score (SS), is presented in Figure 4.5. Entropy of these indicators with corresponding assigned weight are shown in Figure 4.6. Comparatively, higher entropy was estimated for CC and SS, consequently, these indicators were assigned smaller weights contrary to NRMSD which was assigned higher weights.

In the evaluation of precipitation estimates (PEs) at the monthly scale, IMDAA consistently ranked lowest for most stations, with the exception of two stations where it achieved the top rank across all MCDM methods (Figure 4.7). In contrast to the daily time series analysis, where IMD and ERA5 dominated in terms of performance ranking, IMERG exhibited an improved performance in the monthly analysis by achieving rank 1 and rank 2 for significant number of stations . Nevertheless, the variation in rankings produced by different MCDM techniques highlights the need for integrating these rankings to enhance the robustness of

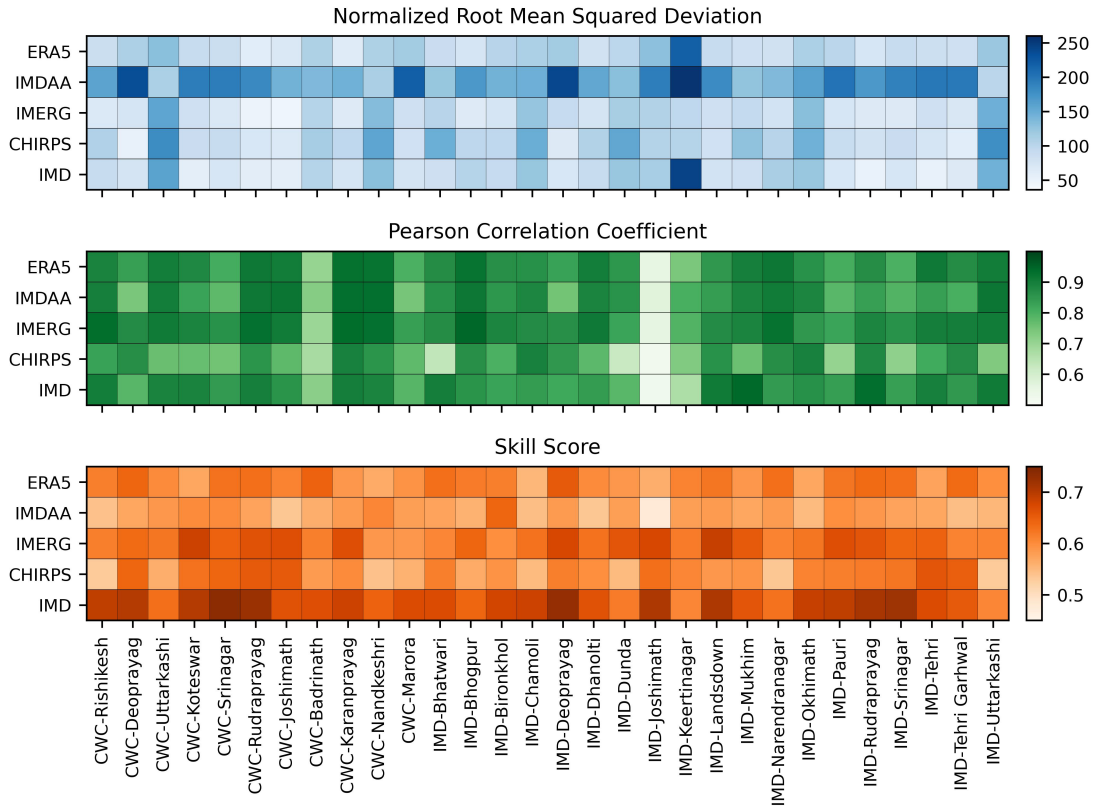

Figure 4.5: Performance indicator for monthly time series.

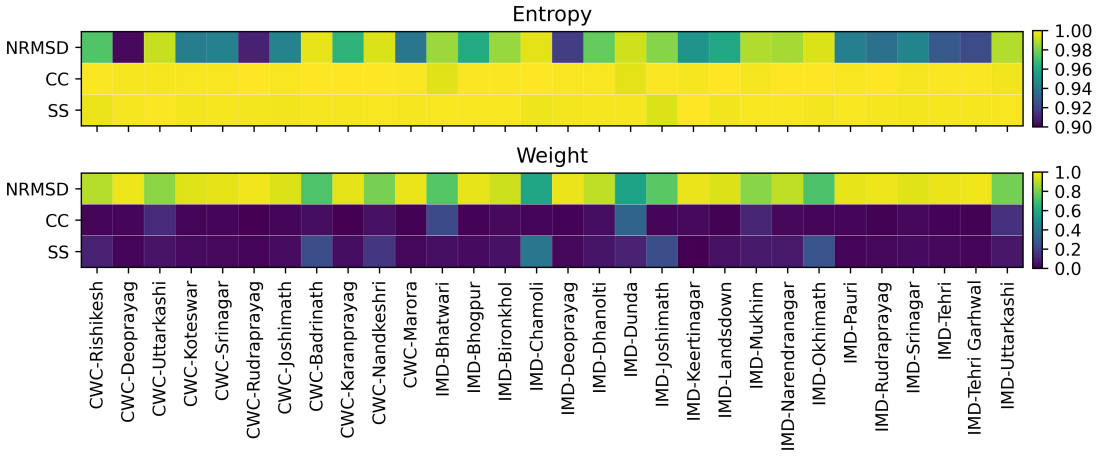

Figure 4.6: Entropy value and weight assigned to performance indicators for computing performance ranking employing daily time series.

decision-making.

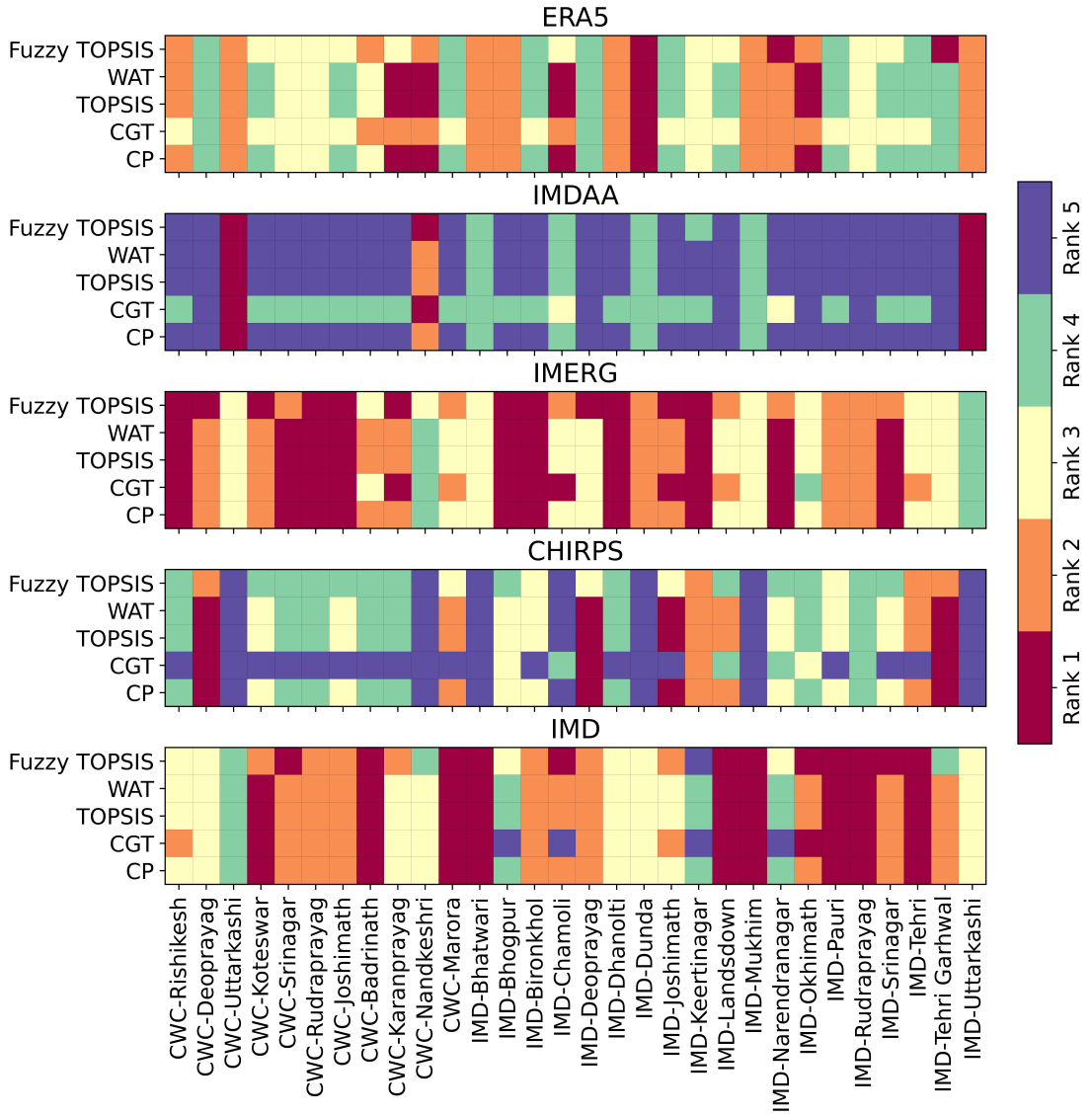

Figure 4.7: Performance ranking of PEs employing monthly time series and different MCDM techniques.

4.2.3 MCDM based performance ranking using monthwise time series

After estimating the performance ranking of PEs by analysing daily (section 4.2.1) and monthly time series (section 4.2.2), further analysis was performed for monthwise time series. In monthwise time series, daily data was arranged monthwise for each grid, and daily estimates of PEs for specific months (e.g., July) were evaluated using the corresponding month of station data (i.e., July). In monthwise analysis, the entropy and weights were computed for each months for each stations (performance indicators not shown here) to apply in MCDM ranking methods. The entropy of various performance indicators for different months of the year is presented in Figure 4.8. These entropy values were further used to assign weights to the indicators (Figure 4.9) for their subsequent use in the MCDM methods, similar to the approach applied to the daily and monthly series.

An illustration for the month of July is presented herein to show how the each PE has performed during ranking (Figure 4.10). Notably, with few exceptions, the ranks assigned to a particular PE varied across different MCDM methods. Significant variability in the performance ranks of PEs was observed across several stations, as determined by the different MCDM approaches. To derive definitive conclusions, the integration of rankings using the GDM is essential. For the selected case of July, the IMDAA dataset consistently received the lowest rankings across the majority of stations from all the applied MCDM techniques. In contrast, ERA5, another reanalysis product, demonstrated significantly better performance, as reflected in its comparatively higher rankings assigned by the MCDM methods. Between IMERG and CHIRPS, IMERG exhibited superior performance, as it was not ranked lowest at any station by any MCDM technique. Conversely, CHIRPS was ranked lowest at multiple stations across different MCDM methods, indicating its comparatively lower skill.

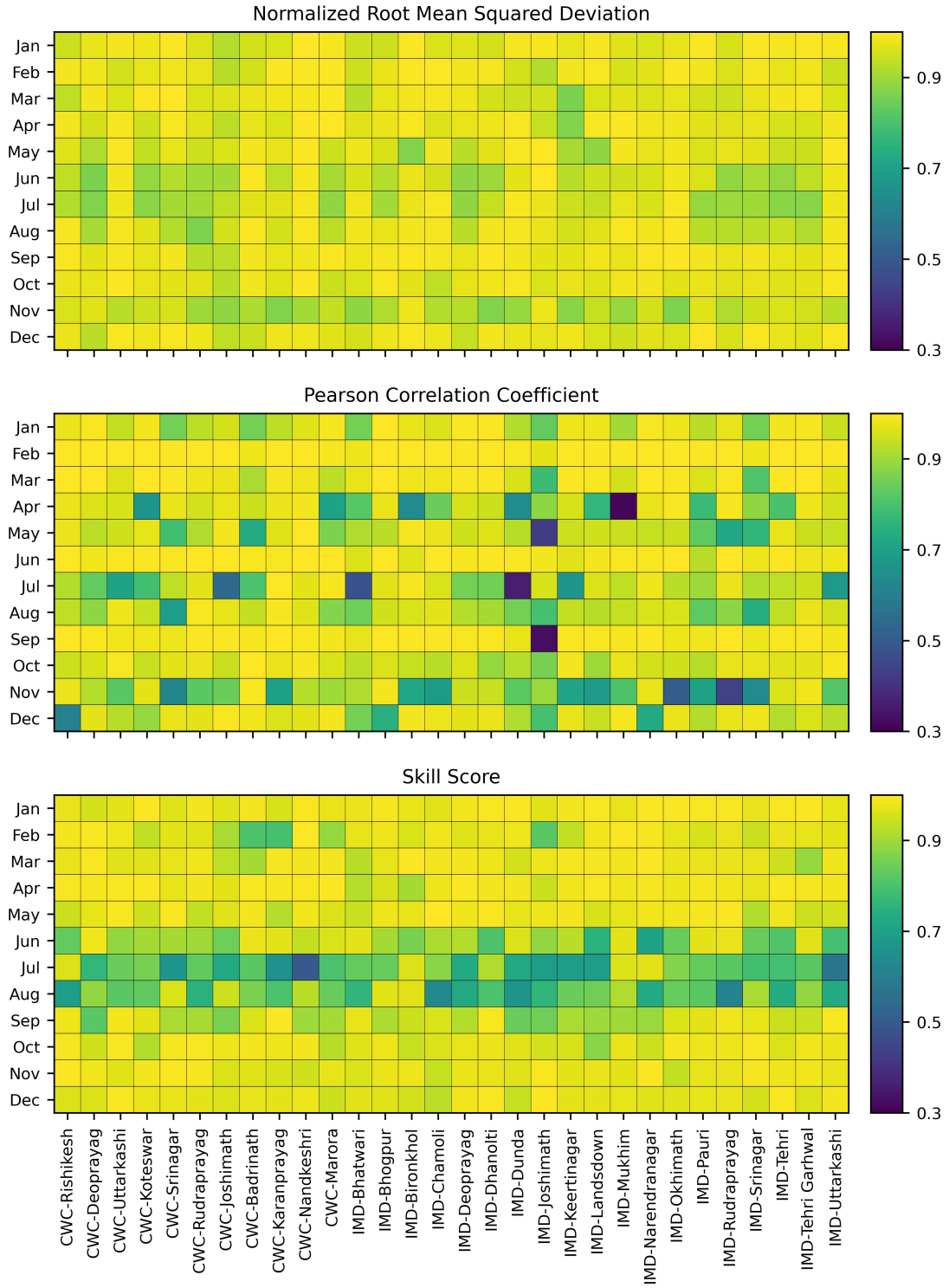

Figure 4.8: Entropy of performance indicators for computing performance ranking employing monthly time series.

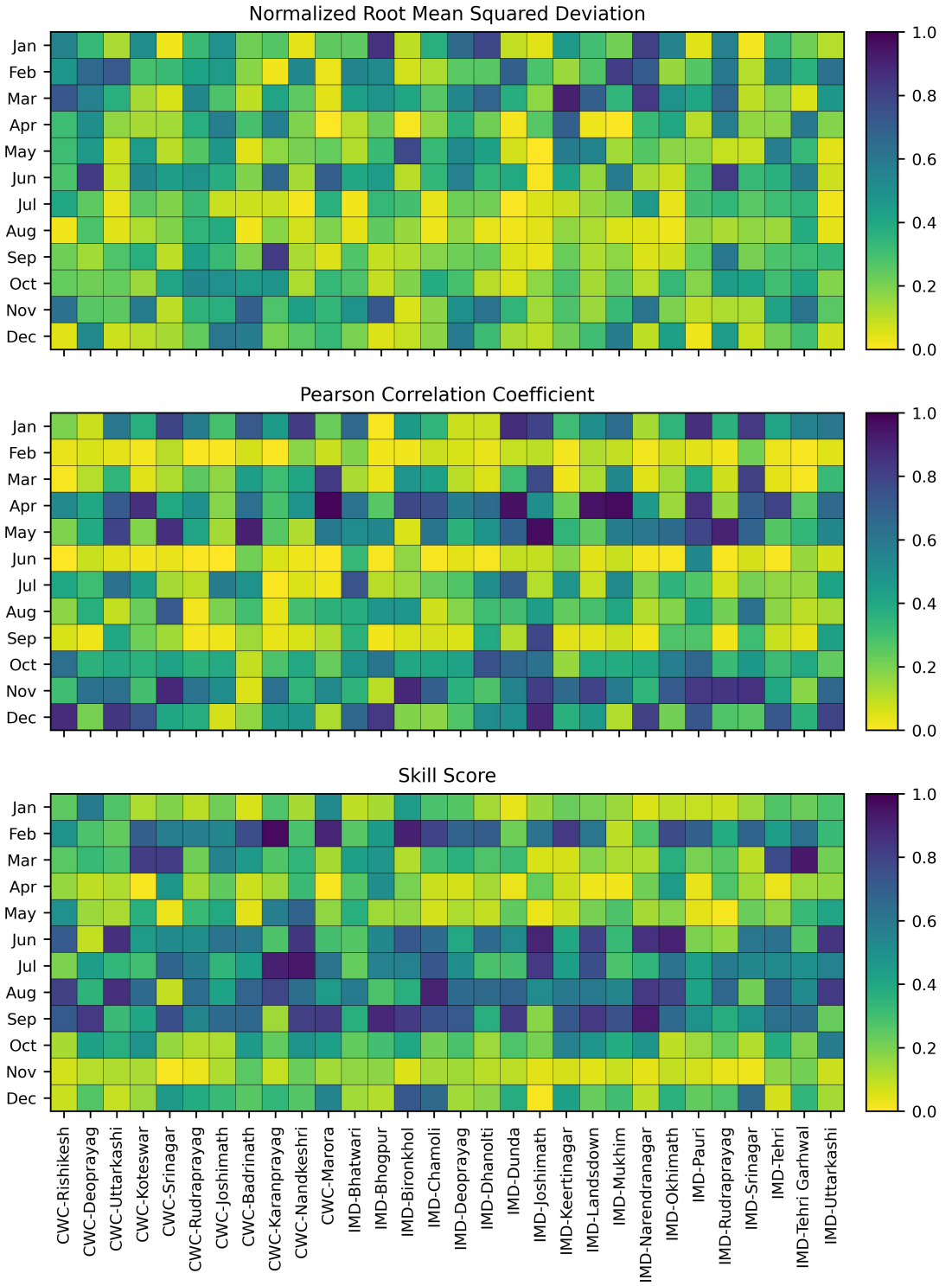

Figure 4.9: Weight assigned to performance indicators for computing performance ranking employing monthly time series.

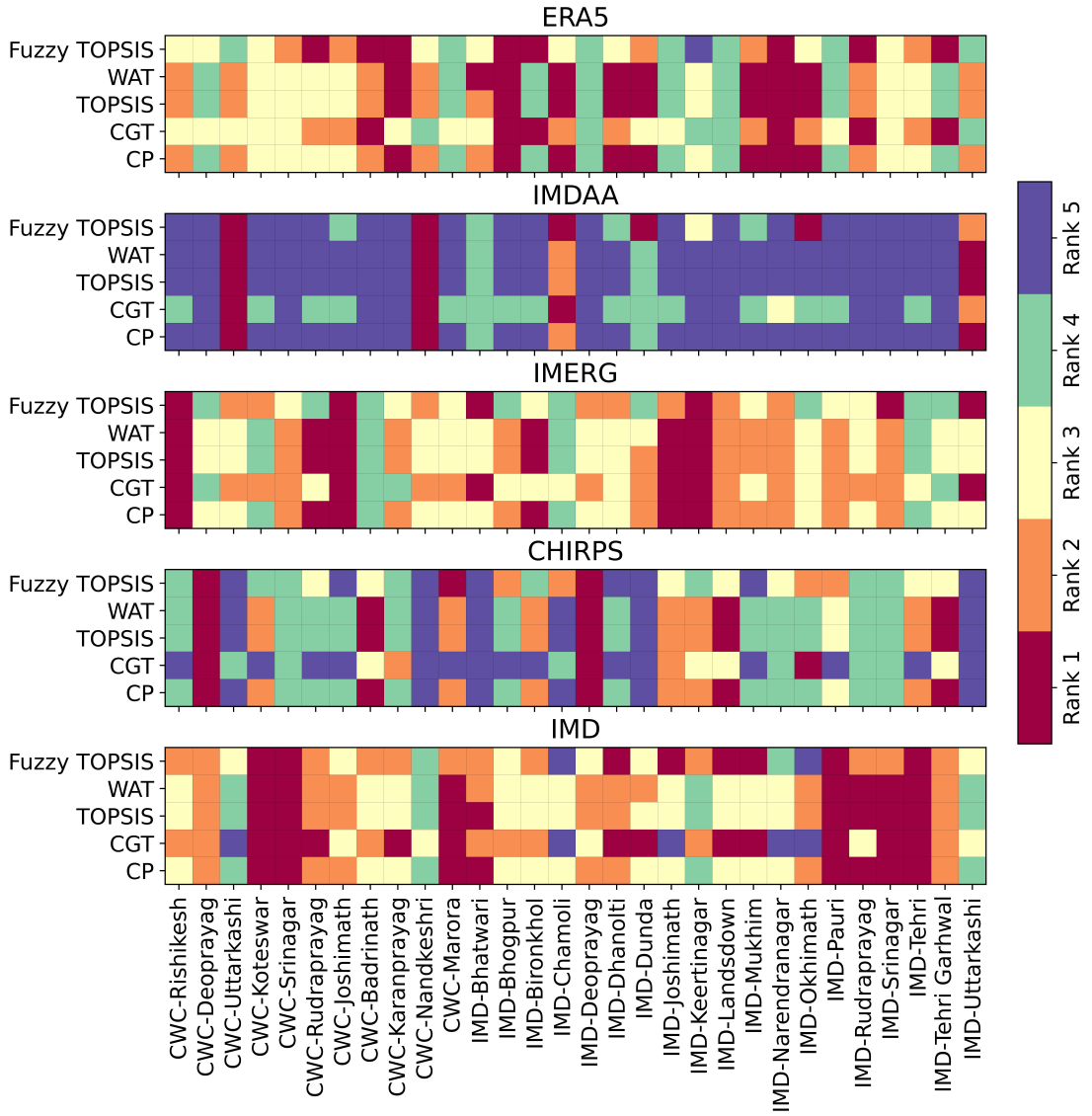

Figure 4.10: Performance ranking of PEs employing monthwise time series and different MCDM techniques for the month of July.

4.3 Integration of performance ranking using GDM approach

As discussed in the previous sections, owing to the ambiguous results yielded by different MCDM methods for a specific PE over a specific grid, it is imperative to integrate the results of different approaches to make a conclusive and informed decision. Therefore, the performance ranks of all the PEs were integrated to derive a final rank utilizing the spearman correlation coefficient and additive ranking rule as explained in section 3.2.5.1 and section 3.2.5.2.

In following sections, station-wise integration of PEs' ranks obtained using daily time series, monthly time series, and monthwise time series are presented.

4.3.1 Integration of performance ranking obtained using daily time series

For daily time series, IMD is found to outrank all other PEs wherein for all the stations, except four (i.e., CWC-Sringar, IMD-Sringar, IMD-Dhanolti, and IMD-Keertinagar), it obtained rank 1 in GDM approach (4.11). However, for IMD it was an obvious outcome as all the methods ranked it 1 in MCDM analysis (Figure 4.4), furthermore, IMD gridded data is also developed using the station record hence, it is expected to match well with the station record when evaluated against the longer station time series. In other PEs, i.e., ERA5, IMDAA, CHIRPS, and IMERG; ERA5 was found to perform better than other PEs for all the stations except CWC-Srinagar, IMD-Sringar, and IMD-Pauri. In contrast, IMDAA, another reanalysis PE showed lower performance.

Count of specific ranks attained by the individual PEs are further tabulated in Table 4.1.

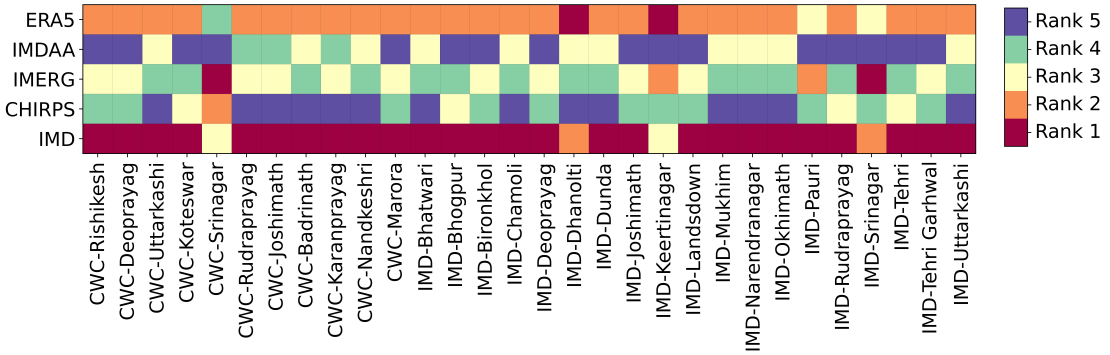

Figure 4.11: Color matrix of performance ranking of PEs after applying GDM for daily time series.

Table 4.1: Station counts versus PEs' ranking for daily time series

	Rank 1	Rank 2	Rank 3	Rank 4	Rank 5
ERA5	2	25	2	1	0
IMDAA	0	0	11	3	16
IMERG	2	2	11	15	0
CHIRPS	0	1	4	11	14
IMD	26	2	2	0	0

4.3.2 Integration of performance ranking obtained using monthly time series

Consistent with the analysis of daily precipitation time series presented earlier, the IMDAA was identified as the least suitable for the Upper Ganga Basin (UGB). This finding is substantiated by its ranking as the lowest-performing PE for 23 out of the 30 evaluated stations (Figure 4.13, Table 4.2). Conversely, for the monthly time series, IMERG demonstrated the highest accuracy among the analyzed PEs, achieving top rankings for 21 stations and never being ranked last for any station.

Following IMERG, ERA5 and the IMD gridded datasets exhibited good

performance. The IMD dataset was ranked first for 9 stations and second for 8 stations, underscoring its consistent reliability across the study area. In contrast, the IMDAA and CHIRPS datasets were ranked significantly lower, reinforcing their classification as the least suitable PEs for monthly time series analysis in the UGB.

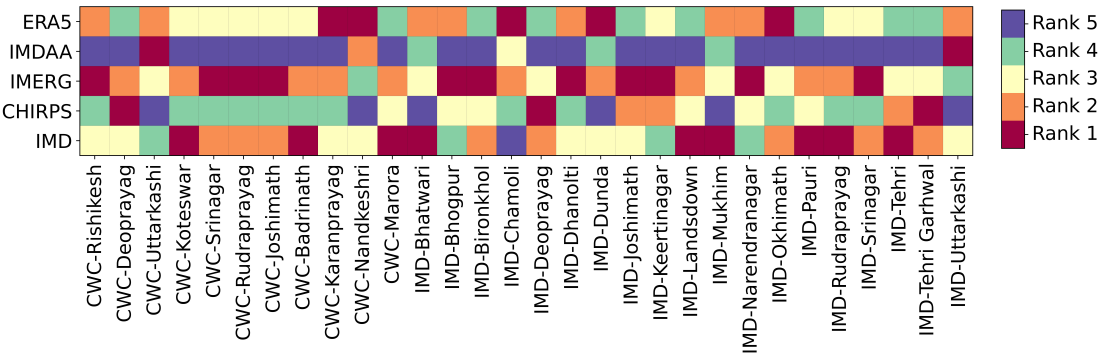

Figure 4.12: Color matrix of performance ranking of PEs after applying GDM for monthly time series.

Table 4.2: Station counts versus PEs' ranking for monthly time series

	Rank 1	Rank 2	Rank 3	Rank 4	Rank 5
ERA5	5	8	8	9	0
IMDAA	2	1	1	3	23
IMERG	11	10	7	2	0
CHIRPS	3	3	6	12	6
IMD	9	8	8	4	1

4.3.3 Integration of performance ranking obtained using monthwise time series

Similar to the integration of PE rankings using the GDM approach for daily and monthly time series, rankings for individual months were also integrated to derive

conclusive inferences. The analysis revealed that IMD, IMERG, and ERA5 consistently demonstrated superior performance across various months of the year. IMD gridded data achieved the first or second rank for the highest number of stations compared to other PEs (Figure 4.13, Table 4.3). However, during May and June, IMERG and ERA5 outperformed the IMD gridded precipitation estimates. Overall, IMDAA was ranked lowest in the majority of instances, followed by CHIRPS, indicating their limited applicability for hydrological analysis in the Upper Ganga Basin.

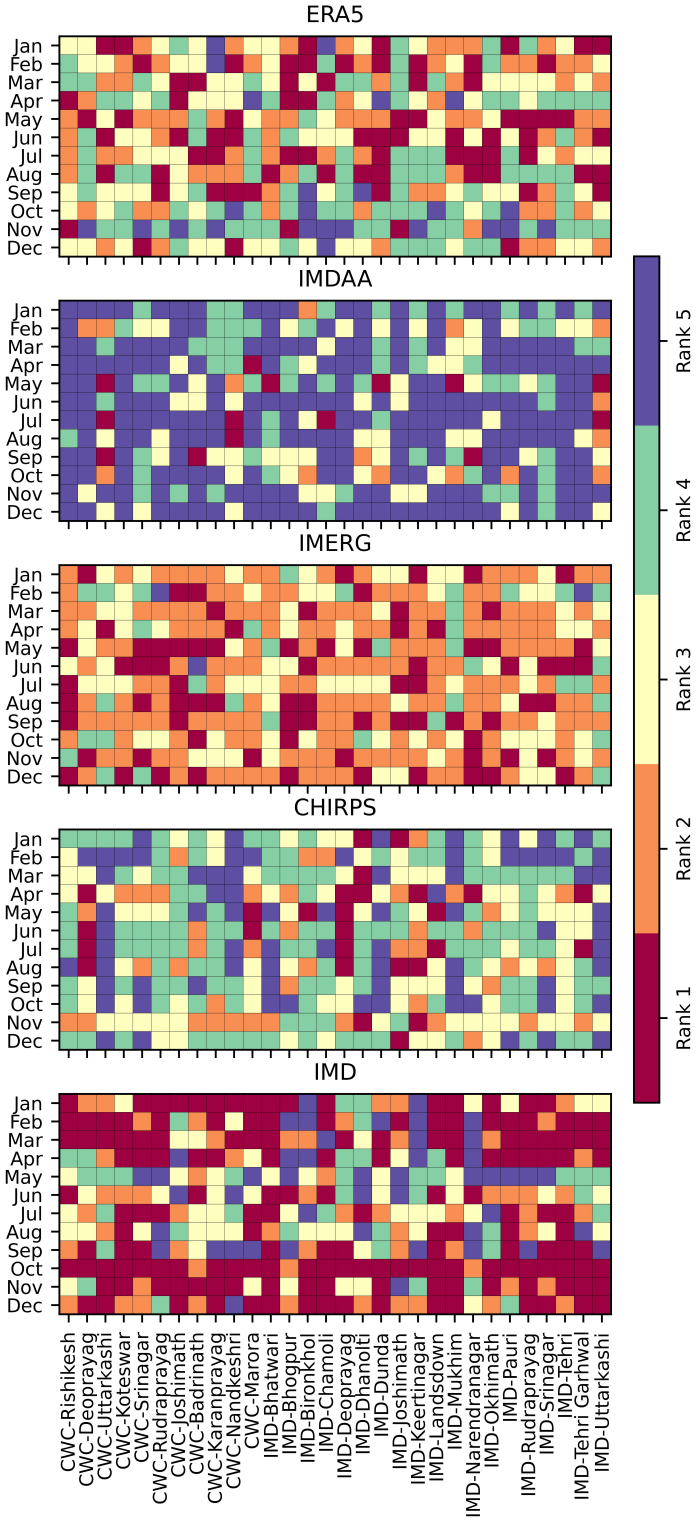

Figure 4.13: Color matrix of performance ranking of PEs for each month after applying GDM for monthwise time series.

Table 4.3: Grid counts versus PEs' ranking for monthwise time series

		Rank 1	Rank 2	Rank 3	Rank 4	Rank 5
Jan	**ERA5**	7	8	9	4	2
	IMDAA	0	1	0	10	19
	IMERG	5	15	9	1	0
	CHIRPS	2	1	7	13	7
	IMD	16	5	5	2	2
Feb	**ERA5**	9	9	7	4	1
	IMDAA	0	4	10	7	9
	IMERG	3	10	7	8	2
	CHIRPS	0	3	5	9	13
	IMD	18	4	1	2	5
Mar	**ERA5**	6	6	10	8	0
	IMDAA	0	0	3	8	19
	IMERG	4	19	6	1	0
	CHIRPS	1	0	8	13	8
	IMD	19	5	3	0	3
Apr	**ERA5**	4	3	8	12	3
	IMDAA	1	0	4	6	19
	IMERG	4	16	7	3	0
	CHIRPS	6	8	9	4	3
	IMD	15	3	2	5	5

May	**ERA5**	9	14	5	2	0
	IMDAA	5	1	4	9	11
	IMERG	12	11	4	3	0
	CHIRPS	4	2	10	6	8
	IMD	0	2	7	10	11
Jun	**ERA5**	11	5	9	5	0
	IMDAA	0	1	5	2	22
	IMERG	9	12	6	2	1
	CHIRPS	3	4	2	18	3
	IMD	7	8	8	3	4
Jul	**ERA5**	9	8	6	7	0
	IMDAA	4	0	2	2	22
	IMERG	4	11	12	3	0
	CHIRPS	4	4	2	14	6
	IMD	9	7	8	4	2
Aug	**ERA5**	10	6	1	13	0
	IMDAA	1	1	7	2	19
	IMERG	9	14	3	4	0
	CHIRPS	4	5	7	7	7
	IMD	6	4	12	4	4

Sep	**ERA5**	7	4	10	7	2
	IMDAA	3	1	9	5	12
	IMERG	9	18	1	2	0
	CHIRPS	0	2	8	13	7
	IMD	11	5	2	3	9
Oct	**ERA5**	0	8	5	13	4
	IMDAA	0	6	4	4	16
	IMERG	3	11	12	4	0
	CHIRPS	0	2	9	9	10
	IMD	27	3	0	0	0
Nov	**ERA5**	3	1	0	15	11
	IMDAA	0	0	5	7	18
	IMERG	7	15	7	1	0
	CHIRPS	2	11	13	4	0
	IMD	18	3	5	3	16
Dec	**ERA5**	3	6	13	7	1
	IMDAA	0	0	5	2	23
	IMERG	10	13	4	3	0
	CHIRPS	1	1	7	16	5
	IMD	16	10	1	2	1

The discussions in Sections 4.3.1, 4.3.2, and 4.3.3 demonstrate that the

results of various MCDM techniques can be synthesized into a unified outcome using GDM approaches. It was observed that, while the IMD gridded dataset outperformed other PEs for most stations in the evaluation of daily time series (Table 4.1) and monthwise time series (Table 4.3), other PEs, such as ERA5 and IMERG, showed superior performance at certain stations. This has significant implications for hydrological analyses targeting station-specific responses, as the omission of the best-performing PE could lead to misleading conclusions. IMERG and ERA5 demonstrated superior agreement with station records for monthly time series performance rankings compared to IMD (Table 4.2).

Conversely, at the basin scale—encompassing multiple grids—IMERG or ERA5 may be more suitable, particularly because the IMD gridded data is available at a coarser spatial resolution and may exhibit inherent discrepancies in grids where quality station data is unavailable. These discrepancies could influence the creation of the gridded dataset and impact its reliability.

Moreover, it is important to investigate how different PEs affect the outcomes of hydrological analyses, such as river discharge simulations in hydrological models. Additionally, herein the performance rankings derived from MCDM methods rely on gap-filled station observations as reference data, underscoring the critical role of station data accuracy in determining the overall reliability of the rankings.

Chapter 5

Summary and Conclusions

5.1 Overview

Precipitation is a critical input for hydrological studies aimed at effective water resource management in any region. The Upper Ganga Basin (UGB), home to the Gangotri Glacier and the headwaters of the Ganga and Yamuna rivers, holds particular significance for water resources. With the global hydrological regime undergoing substantial changes, it is imperative to understand the responses of these rivers to climate change and develop decision support systems for sustainable water resource management. However, obtaining reliable precipitation data in the Himalayan region is challenging due to the sparse distribution of rain gauge networks, a consequence of the region's complex topography and harsh climatic conditions. This limitation can be mitigated by leveraging Satellite Precipitation Estimates (SPEs) and Reanalysis Precipitation Estimates (RPEs), which are provided by various international agencies and organizations. In recent years, numerous high-resolution precipitation datasets have been developed, offering promising alternatives for hydrological analyses. Nevertheless, before applying these datasets to a specific region, it is essential to evaluate their performance within the context of the study area to ensure their reliability and suitability.

Keeping above discussion in view, following specific objectives were formulated for this study,

1. To perform statistical evaluation of fine scale satellite and reanalysis precipitation products in Upper Ganga Basin vis-à-vis station records.
2. To estimate performance ranking of fine scale satellite and reanalysis precipitation product in Upper Ganga Basin using Multicriterion Decision-Making and Group Decision-Making.

The primary objective of this study was to assess the ability of various Precipitation Estimates (PEs) to capture the regional precipitation climatology of the Upper Ganga Basin (UGB). The analysis included four very high-resolution PEs, comprising two Satellite Precipitation Estimates (SPEs) — IMERG and CHIRPS — and two Reanalysis Precipitation Estimates (RPEs) — ERA5 and IMDAA (Table 2.2.2). Additionally, a comparatively coarser-resolution IMD gridded dataset, derived from station-based observations and widely regarded as a benchmark dataset, was included for comparative evaluation.

The selected PEs were analyzed for their ability to resolve daily, monthly, and monthwise precipitation patterns across all stations in the UGB. Initially, the precipitation climatology was examined using graphical methods (Section 4.1) to evaluate how the monthly and annual precipitation regimes from different PEs aligned with station-based observations across the basin. To quantify the performance of each PE, Multi-Criteria Decision-Making (MCDM) techniques (Section 4.2) were employed. These methods incorporated Compromise Programming (Section 3.2.3.1), Cooperative Game Theory (Section 3.2.3.2), TOPSIS (Section 3.2.3.3), the Weighted Average Technique (Section 3.2.3.4), and Fuzzy TOPSIS (Section 3.2.4.1).

Performance indicators, including Normalized Root Mean Square Deviation (NRMSD), Pearson Correlation Coefficient (CC), and Skill Score (SS) (Section 3.1), were applied within each MCDM approach. Weights for these indicators were assigned using an entropy-based weighting scheme (Section 3.2.2) to determine

the rank of each PE. Finally, the performance rankings obtained from the different MCDM methods were integrated using the Group Decision-Making (GDM) approach (Section 4.3), which employed the Spearman correlation coefficient (Section 3.2.5.1) and an additive ranking rule (Section 3.2.5.2).

5.2 Conclusions

Based on the analysis carried out following specific conclusion were derived,

1. Among the Precipitation Estimates (PEs) analyzed, IMD, IMERG, and ERA5 exhibit superior skill in capturing the regional precipitation climatology compared to CHIRPS and IMDAA.

2. CHIRPS consistently underestimates the annual precipitation regime.

3. This underestimation by CHIRPS is particularly pronounced during the period from 2000 to 2008, where it systematically recorded lower precipitation than observed. However, its performance improved significantly after 2008, showing better agreement with observations.

4. IMDAA demonstrates a consistent overestimation of annual precipitation across all analyzed years.

5. For daily and monthwise daily precipitation, IMD consistently ranked highest among all PEs for the majority of cases. ERA5 and IMERG also performed well, often emerging as the next best-suited PEs.

6. IMERG exhibited the best performance for monthly precipitation, surpassing all other PEs at most stations.

7. The performance of PEs varied significantly across grids, with different products outperforming one another for specific months in the monthwise daily precipitation analysis.

8. IMDAA and CHIRPS were identified as the least reliable precipitation estimates for the Upper Ganga Basin.

5.3 Challenges and limitations of the study

The evaluation and ranking of selected Precipitation Estimates (PEs) in this study relied on station-based observational data. To address gaps in the observational records, statistical techniques were employed to reconstruct long-term, consistent time series by leveraging data from neighboring stations. However, this approach introduces inherent challenges, as the synthetically generated datasets may not accurately represent the true rainfall characteristics of individual stations. This limitation poses a significant constraint on the reliability of the analysis.

The challenge is particularly pronounced in mountainous regions, where the establishment and maintenance of meteorological stations are logistically complex and financially demanding. Ensuring the continuous operation of these observatories over extended periods requires substantial resources and sustained effort. As a result, filling data gaps through statistical methods becomes an unavoidable necessity in such regions, despite the potential for inaccuracies in capturing localized precipitation variability.

5.4 Contributions and recommendations for future work

The research conducted in this study holds significant practical and scientific relevance. Its findings are expected to provide valuable insights for hydrologists, particularly in the analysis of water resources and the response of river basins to climate change within the Upper Ganga Basin (UGB). This study makes two key contributions:

1. While numerous studies have assessed Precipitation Estimates (PEs) in the Indian Himalayan Region (IHR), there has been a lack of in-depth analysis focused on very fine-resolution PEs using an extensive network of meteorological stations. This gap was addressed herein, particularly, for the UGB.

2. The application of Multi-Criteria Decision-Making (MCDM) techniques enables the integration of various performance indicators, providing a systematic framework for ranking precipitation products. In contrast, Group Decision-Making (GDM) approaches aggregate these rankings by assigning appropriate weights to each MCDM method, thus facilitating a comprehensive evaluation. The methodology employed in this study ensures that the results are both robust and reliable, offering a level of confidence that can support informed decision-making by researchers and water resource managers.

The limitations and challenges encountered in this research present opportunities for refining the results and gaining deeper insights into the findings. The following four recommendations are proposed for future research endeavors to address these challenges and enhance the robustness of the analysis:

1. The results of this study may not be universally applicable to other regions due to the inherently spatially heterogeneous nature of precipitation patterns. Consequently, future research could expand the scope of this analysis to other river basins, assessing the effectiveness of various PEs in capturing regional climatological characteristics. Such extensions would help to determine the broader applicability and robustness of the findings in diverse geographical contexts.

2. To enhance the robustness of performance evaluations, additional performance indicators could be incorporated into the Multi-Criteria Decision-Making (MCDM) framework, thereby refining the ranking of different PEs.

References

Andermann, C., Bonnet, S., & Gloaguen, R. (2011). Evaluation of precipitation data sets along the himalayan front. *Geochemistry, Geophysics, Geosystems*, *12*(7).

Arora, M., Singh, P., Goel, N., & Singh, R. (2006). Spatial distribution and seasonal variability of rainfall in a mountainous basin in the himalayan region. *Water Resources Management*, *20*(4), 489–508.

Banerjee, A., Dimri, A., & Kumar, K. (2020). Rainfall over the himalayan foot-hill region: present and future. *Journal of Earth System Science*, *129*(1), 1–16.

Basistha, A., Arya, D. S., & Goel, N. K. (2008). Spatial distribution of rainfall in indian himalayas–a case study of uttarakhand region. *Water Resources Management*, *22*, 1325–1346.

Beria, H., Nanda, T., Singh Bisht, D., & Chatterjee, C. (2017). Does the gpm mission improve the systematic error component in satellite rainfall estimates over trmm? an evaluation at a pan-india scale. *Hydrology and Earth System Sciences*, *21*(12), 6117–6134.

Bhattacharyya, S., Sreekesh, S., & King, A. (2022). Characteristics of extreme rainfall in different gridded datasets over india during 1983–2015. *Atmospheric Research*, *267*, 105930.

Bhutiyani, M., Kale, V. S., & Pawar, N. (2007). Long-term trends in maximum, minimum and mean annual air temperatures across the northwestern himalaya during the twentieth century. *Climatic Change*, *85*(1), 159–177.

Bisht, D. S., Chatterjee, C., Raghuwanshi, N. S., & Sridhar, V. (2018). Spatio-temporal trends of rainfall across indian river basins. *Theoretical and applied climatology*, *132*(1), 419–436.

Bisht, D. S., Chowdhury, B., Rawat, S. S., & Pottakkal, J. G. (2024). Performance ranking of global precipitation estimates over data scarce western himalayan region of india. *Theoretical and Applied Climatology*, (pp. 1–23).

Bisht, D. S., Sridhar, V., Mishra, A., Chatterjee, C., & Raghuwanshi, N. S. (2019). Drought characterization over india under projected climate scenario. *International Journal of Climatology*, *39*(4), 1889–1911.

Bookhagen, B., & Burbank, D. W. (2010). Toward a complete himalayan hydrological budget: Spatiotemporal distribution of snowmelt and rainfall and their impact on river discharge. *Journal of Geophysical Research: Earth Surface*, *115*(F3).

Cavalcante, R. B. L., da Silva Ferreira, D. B., Pontes, P. R. M., Tedeschi, R. G., da Costa, C. P. W., & de Souza, E. B. (2020). Evaluation of extreme rainfall indices from chirps precipitation estimates over the brazilian amazonia. *Atmospheric Research*, *238*, 104879.

Chowdhury, B., Goel, N. K., & Arora, M. (2021). Evaluation and ranking of different gridded precipitation datasets for satluj river basin using compromise programming and f-topsis. *Theoretical and Applied Climatology*, *143*, 101–114.

Connolly, T. G., & Sluckin, W. (1971). *Introduction to statistics for the social sciences*. Springer.

Consultants, D., & Hydraulics, D. (1999). Surface water data entry system (swdes) – users' manual. Technical report. Technical assistance under Hydrology Project - I.

Cui, W., Dong, X., Xi, B., Feng, Z., & Fan, J. (2020). Can the gpm imerg final product accurately represent mcss' precipitation characteristics over the central and eastern united states? *Journal of Hydrometeorology*, *21*(1), 39–57.

Dimri, A., & Dash, S. (2012). Wintertime climatic trends in the western himalayas. *Climatic Change*, *111*(3), 775–800.

Funk, C., Peterson, P., Landsfeld, M., Pedreros, D., Verdin, J., Shukla, S., Husak, G., Rowland, J., Harrison, L., Hoell, A., et al. (2015). The climate hazards infrared precipitation with stations—a new environmental record for monitoring extremes. *Scientific data*, *2*(1), 1–21.

Gershon, M., & Duckstein, L. (1983). Multiobjective approaches to river basin planning. *Journal of Water Resources Planning and Management*, *109*(1), 13–28.

Gibbons, J. D., & Chakraborti, S. (2014). *Nonparametric statistical inference*. CRC press.

Huffman, G. J., Bolvin, D. T., Nelkin, E. J., & Tan, J. (2015). Integrated multi-satellite retrievals for gpm (imerg) technical documentation. *Nasa/Gsfc Code*, *612*(47), 2019.

Hydraulics, D. (1999). Hymos manual, version 4.01. Technical report, Delft Hydraulics. Technical assistance under Hydrology Project - I.

IPCC (2023). Summary for Policymakers. In: Climate Change 2023: Synthesis Report. Contribution of Working Groups I, II and III to the Sixth Assessment Report of the Intergovernmental Panel on Climate Change [Core Writing Team, H. Lee and J. Romero (eds.)]. *IPCC, Geneva, Switzerland*, (pp. 1–34).

Li, X., Sungmin, O., Wang, N., Huang, Y., et al. (2021). Evaluation of the gpm imerg v06 products for light rain over mainland china. *Atmospheric Research*, *253*, 105510.

Meher, J. K., Das, L., Akhter, J., Benestad, R. E., & Mezghani, A. (2017). Performance of cmip3 and cmip5 gcms to simulate observed rainfall characteristics over the western himalayan region. *Journal of Climate*, *30*(19), 7777–7799.

Mishra, P. K., Thayyen, R. J., Singh, H., Das, S., Nema, M. K., & Kumar, P. (2022). Assessment of cloudbursts, extreme rainfall and vulnerable regions in the upper ganga basin, uttarakhand, india. *International Journal of Disaster Risk Reduction*, *69*, 102744.

Morais, D. C., & de Almeida, A. T. (2012). Group decision making on water resources based on analysis of individual rankings. *Omega*, *40*(1), 42–52.

Muñoz-Sabater, J., Dutra, E., Agustí-Panareda, A., Albergel, C., Arduini, G., Balsamo, G., Boussetta, S., Choulga, M., Harrigan, S., Hersbach, H., et al. (2021).

Era5-land: A state-of-the-art global reanalysis dataset for land applications. *Earth system science data*, *13*(9), 4349–4383.

NIH (2022). Integrated hydrological studies for upper ganga basin up to rishikesh. Sponsored by: Department of Science & Technology, Govt. of India.

Opricovic, S., & Tzeng, G.-H. (2004). Compromise solution by mcdm methods: A comparative analysis of vikor and topsis. *European journal of operational research*, *156*(2), 445–455.

Pai, D., Rajeevan, M., Sreejith, O., Mukhopadhyay, B., & Satbha, N. (2014). Development of a new high spatial resolution (0.25× 0.25) long period (1901-2010) daily gridded rainfall data set over india and its comparison with existing data sets over the region. *Mausam*, *65*(1), 1–18.

Palazzi, E., Von Hardenberg, J., & Provenzale, A. (2013). Precipitation in the hindu-kush karakoram himalaya: observations and future scenarios. *Journal of Geophysical Research: Atmospheres*, *118*(1), 85–100.

Pomerol, J.-C., & Barba-Romero, S. (2000). *Multicriterion decision in management: principles and practice*, vol. 25. Springer Science & Business Media.

Rani, S. I., Arulalan, T., George, J. P., Rajagopal, E., Renshaw, R., Maycock, A., Barker, D. M., & Rajeevan, M. (2021). Imdaa: High-resolution satellite-era reanalysis for the indian monsoon region. *Journal of Climate*, *34*(12), 5109–5133.

Shukla, A. K., Ojha, C. S. P., Singh, R. P., Pal, L., & Fu, D. (2019). Evaluation of trmm precipitation dataset over himalayan catchment: the upper ganga basin, india. *Water*, *11*(3), 613.

Singh, J., Yadav, R. R., & Wilmking, M. (2009). A 694-year tree-ring based rainfall reconstruction from himachal pradesh, india. *Climate Dynamics*, *33*(7), 1149–1158.

Singh, P., Ramasastri, K., & Kumar, N. (1995). Topographical influence on precipitation distribution in different ranges of western himalayas. *Hydrology Research*, *26*(4-5), 259–284.

Singh, T., Saha, U., Prasad, V., & Gupta, M. D. (2021). Assessment of newly-developed high resolution reanalyses (imdaa, ngfs and era5) against rainfall observations for indian region. *Atmospheric Research*, *259*, 105679.

Singh, V. P., Singh, R., Paul, P. K., Bisht, D. S., & Gaur, S. (2024). Data availability and aquisition. In *Hydrological Processes Modelling and Data Analysis: A Primer*, (pp. 13–34). Springer.

Srinivasa Raju, K., & Nagesh Kumar, D. (2010). *Multicriterion analysis in engineering and management*. PHI Learning Pvt. Ltd.

Srinivasa Raju, K., & Nagesh Kumar, D. (2015a). Fuzzy approach to rank global climate models. In *Proceedings of the Fifth International Conference on Fuzzy and Neuro Computing (FANCCO-2015)*, (pp. 53–61). Springer.

Srinivasa Raju, K., & Nagesh Kumar, D. (2015b). Ranking general circulation models for india using topsis. *Journal of Water and Climate Change*, *6*(2), 288–299.

Srinivasa Raju, K., Sonali, P., & Nagesh Kumar, D. (2017). Ranking of cmip5-based global climate models for india using compromise programming. *Theoretical and applied climatology*, *128*(3), 563–574.

Wang, M., Rezaie-Balf, M., Naganna, S. R., & Yaseen, Z. M. (2021). Sourcing chirps precipitation data for streamflow forecasting using intrinsic time-scale decomposition based machine learning models. *Hydrological Sciences Journal*, *66*(9), 1437–1456.

Yadav, B. C., Thayyen, R. J., & Jain, K. (2020). Topoclimatic zones and characteristics of the upper ganga basin, uttarakhand, india. *International Journal of Climatology*, *40*(14), 6002–6019.

Yang, T., & Hung, C.-C. (2007). Multiple-attribute decision making methods for plant layout design problem. *Robotics and computer-integrated manufacturing*, *23*(1), 126–137.

Yu, C., Hu, D., Duan, X., Zhang, Y., Liu, M., & Wang, S. (2020a). Rainfall-runoff simulation and flood dynamic monitoring based on chirps and modis-et. *International Journal of Remote Sensing*, *41*(11), 4206–4225.

Yu, C., Hu, D., Liu, M., Wang, S., & Di, Y. (2020b). Spatio-temporal accuracy evaluation of three high-resolution satellite precipitation products in china area. *Atmospheric research*, *241*, 104952.